Title

Longitudinal Control Development For IVHS Fully Automated And Semi - Automated System: Phase III

Authors
Hedrick, J. K.
Garg, V.
Gerdes, J. C.
et al.

Publication Date
1997

CALIFORNIA PATH PROGRAM
INSTITUTE OF TRANSPORTATION STUDIES
UNIVERSITY OF CALIFORNIA, BERKELEY

Longitudinal Control Development for IVHS Fully Automated and Semi-Automated System: Phase III

J.K. Hedrick, V. Garg, J.C. Gerdes,
D.B Maciuca, D. Swaroop
Universtiy of California, Berkeley

California PATH Research Report
UCB-ITS-PRR-97-20

This work was performed as part of the California PATH Program of the University of California, in cooperation with the State of California Business, Transportation, and Housing Agency, Department of Transportation; and the United States Department of Transportation, Federal Highway Administration.

Report for MOU 101

May 1997

ISSN 1055-1425

CALIFORNIA PARTNERS FOR ADVANCED TRANSIT AND HIGHWAYS

This paper uses Postscript Type 3 fonts. Although reading it on the screen is difficult it will print out just fine.

Longitudinal Control Development for IVHS Fully Automated and Semi-Automated System Phase III

Final Report

Submitted to: PATH (MOU 101)

J.K. Hedrick
V. Garg
J.C. Gerdes
D.B. Maciuca
D. Swaroop

Mechanical Engineering Department
University of California at Berkeley
Berkeley, CA 94720-1740

Abstract

This report presents the concluding findings of a three year project concerned with the longitudinal issues regarding modeling and control of vehicles in an Intelligent Vehicles and Highway Systems (IVHS) environment. Specifically, the report addresses the issue of vehicle control in an automated highway system, brake actuation and brake control. Recent research findings in the area of automated vehicle platooning on isolated lanes of an automated highway are included. Performance specifications, control system architecture, vehicle control algorithms, actuator and sensor specifications and communication requirements are also addressed. The issue of switching from throttle to brake actuation is addressed in detail.

Brake actuation does not admit the obvious retrofit solution that exists for engine control (namely, throttle actuation). Possible brake actuation schemes - from pedal actuation to direct control of pressure at each wheel - raise an interesting trade-off between ease of retrofit and ease of control. Obviously, retaining more components of the existing system aids in retrofitting, but trying to automate systems designed for human operation can create serious control problems. An examination of how various actuation strategies can be evaluated in terms of the often conflicting requirements of tracking accuracy and passenger comfort to provide guidelines for both hardware design and future simulation is provided.

The new fluidic model of the brake system provided an avenue for developing a better brake controller. Due to the nonlinearities present in the system, a nonlinear controller was employed. It takes full advantage of the dynamic equations describing the master cylinder and brake hydraulics. Simulations and experimental results were used to confirm its superiority over the previous actuation system and controller.

Experimental results show that the closed-loop system is capable of tracking velociti profiles within 0.1m/s and following a maneuvering lead vehicle at a distance of 2 meters with only 20cm error.

Keywords: IVHS, AHS, AVCS, Longitudinal Control, Brake Control, Braking.

Executive Summary

The problems of traffic congestion and safety are becoming more and more critical in almost all metropolitan areas around the world. Many approaches are and have been taken to alleviate this problem including new freeway construction, new public transit facilities, flexible and overlapping working hours, and more recently the use of intelligent transportation systems (ITS).

In the broad sense, ITS is the use of modern technological advances to provide increased traffic flow and to reduce traffic accidents. Examples of ITS include sensors that provide flow and incident information to roadway management authorities and to the drivers, computerized traffic lights and freeway ramp metering dependent on current conditions and in-vehicle communication and information displays. More recently there have been research programs in the US, Europe and Japan to look at various aspects of vehicle automation, ranging from "Intelligent Cruise Control (ICC)" systems that regulate the throttle and possibly the brake to keep a specific distance between the controlled vehicle and the vehicle in front of it, to fully automated highway systems (AHS) where both lateral and longitudinal control is provided automatically. The University of California, PATH program has concentrated on this area of ITS and recently joined with several US industries and universities to form the National Automated Highway System Consortia (NAHSC). This consortia is currently investigating alternative AHS scenarios and will be narrowing down these possibilities after extensive analysis and field testing. This paper will focus on one of these possibilities, the concept of "platooning" or "convoying" where all vehicles are operated under automated vehicle control.

The concept of controller design for automated highway vehicles has been the focus of a considerable amount of recent research (see, for example, (Chien and Ioannou, 1992; Hedrick *et al.*, 1991; Ren and Green, 1994)). As befits the youthful nature of the field, much of the work to date has centered around control strategies for idealized vehicle models, particularly with respect to brake dynamics. However, brake actuation does not admit the obvious retrofit solution that exists for engine control (namely, throttle actuation). Possible brake actuation schemes - from pedal actuation to direct control of pressure at each wheel - raise an interesting trade-off between ease of retrofit and ease of control. Obviously, retaining more components of the existing system aids in retrofitting, but trying to automate systems designed

for human operation can create serious control problems. Various actuation strategies can be evaluated in terms of the often conflicting requirements of tracking accuracy and passenger comfort to provide guidelines for both hardware design and future simulation.

An actuation scheme which mimics human actions includes the dynamics of the linkage inertia, vacuum assist, master cylinder, brake lines and brakes. Recent work has produced detailed dynamic models of these components along with their associated control problems (Gerdes, 1996). Of these, the most crucial problems have been found to be the dead zones and internal feedback of the vacuum assist, the filling properties of the wheel cylinders and the variable gain of the brake pads. Instead of focusing on particular model-based control strategies, for this study, the various components were abstracted into linear dynamics with uncertainties, dead zones and transport lag. Such an approach makes the inherent control difficulties associated with different actuation strategies a clear function of the components incorporated. Sufficient accuracy is retained, however, to ensure that the results may be applied to actual system components.

The system chosen for this simulation study was that of a vehicle platoon under a sliding control scheme (Hedrick *et al.*, 1991). The vehicles were assumed to incorporate knowledge of the velocity and acceleration of both the preceding car and the lead vehicle of the platoon into the control law. In order to quantify the performance, measures of spacing errors between subsequent vehicles were examined in conjunction with the passenger comfort criteria of acceleration and jerk limits as the platoon executed a representative maneuver. The results of these simulations proved to be quite dramatic. While the controller structure exhibited a certain robustness to the uncertain gain (consistent with design), the presence of delays in the brake dynamics produced catastrophic effects.

With the controller gains fixed at established values, a 40ms delay resulted in poor ride quality by the seventh car in the platoon, as evidenced by substantial jerk. Furthermore, this delay also prevented spacing errors from decreasing uniformly down the platoon. A delay of 80ms resulted in a complete loss of string stability, causing errors to increase with successive vehicles. Simulations further showed that in order to overcome such difficulties, either the bandwidth of the controller (and hence the highway system as a whole) had to be reduced substantially or the platoons had to be limited in size. Since the system bandwidth and platoon size are both factors determining capacity, a small delay in the brake system thus creates large changes in highway performance. Analysis of the presence of a deadzone nonlinearity produced similar qualitative results. Of course, the argument may be made that these results are merely indicative of the particular control scheme chosen. However, this proves in a some sense to be a "best-case scenario" as simulations without lead vehicle information exhibit even greater sensitivity to actuation delay.

Therefore, the choice of brake actuation strategy essentially fixes the trade-off between passenger comfort and system responsiveness. To simultaneously maintain ride quality and string stability, the system bandwidth must vary inversely with the magnitude of any transport lags in the actuation system. Returning to the subject of individual brake components, these results clearly necessitate considerable redesign of existing braking systems for incorporation in an IVHS structure. In contrast to engine control, brake actuation cannot effectively be conceptualized as an automated version of human inputs. Rather, the input must be placed much farther downstream (bypassing the vacuum assist and perhaps master cylinder) to avoid catastrophic dead zones or transport lags. A brief treatment of the design implications of this result and current research into brake actuation at U.C. Berkeley are also presented.

Various aspects of brake control development, from actuator design to performance guarantees to experimental validation of the closed-loop system are also discussed. Implementation of the solution chosen for this work - a separate hydraulic system with an actuator mounted in series between the vacuum booster and master cylinder - is considered and this method compared to modulation of an Anti-Lock Braking System (ABS) or Traction Control System (TCS). A sliding controller capable of fast, accurate pressure control is developed. To avoid problems in implementation, however, modification of the basic structure is required. Proofs are provided to show that the resulting controller is stable.

Contents

Abstract **ii**

Executive Summary **iii**

1 Introduction **1**

2 Vehicle Control in Automated Highway Systems **2**
2.1 Introduction 2
2.2 Performance Specifications 3
2.3 Control System Architecture 4
2.4 Vehicle Control Algorithms 8
2.5 Actuator and Sensor Specification 9
2.5.1 Actuators 9
2.5.2 Sensors 9
2.6 Communication Requirements 10
2.7 Experimental Results 10

3 Brake Actuation Requirements **12**
3.1 Introduction 12
3.2 Vehicle Model and Controller 13
3.2.1 Throttle Control Development 13
3.2.2 Brake Control Development 15
3.2.3 Controller Integration 16
3.3 Simulation Results 18
3.3.1 Methodology 18
3.3.2 Vacuum Booster 19
3.3.3 Torque Feedback 21

3.3.4 Actuator Dynamics 22

4 Brake Control Development **25**

4.1 Actuator Design 26
4.2 Sliding Controller Design 28
4.3 Performance Guarantees 32
4.3.1 Error Dynamics 34
4.3.2 Robustness 36
4.3.3 Estimating t_s 38
4.4 Saturated Sliding Controller 41
4.5 Simulation Results 42
4.6 Experimental Results 45

5 Conclusions **50**

Bibliography **51**

List of Figures

2.1 Impact Velocity vs. Initial Separation 4
2.2 Lane Capacity vs. Platoon Size 5
2.3 PATH Control System Architecture 6

3.1 Brake System Components 12
3.2 Comparison of Switching Rules 16
3.3 Effects of Booster Cut-in Force 19
3.4 Effects of Braking With Threshold 20
3.5 Performance With Brake Gain Mismatch 21
3.6 Effects of 80 Millisecond Delay 22
3.7 Effect of Sliding Gain on Spacing Errors 23

4.1 Direct Master Cylinder Actuation System 26
4.2 Experimental Data for Brake Torque vs. Brake Pressure . . . 28
4.3 Brake Fluid Capacity Curve Used for Controller Design 28
4.4 Trajectory Producing Maximum t_s 38
4.5 Simulated Performance: 1ms Update (Desired - dashed, Actual - solid) 42
4.6 Simulated Performance: 5ms Update (Desired - dashed, Actual - solid) 43
4.7 Control Activity with 5ms Controller Update 44
4.8 Simulated Performance: Uncertainty (Desired - dashed, Actual - solid) 45
4.9 Experimental Controller Performance (Desired - dashed, Actual - solid) 46
4.10 Control Activity During Tracking 47

List of Tables

2.1 Vehicle Range Sensor Specifications 9

4.1 Brake Hydraulic Parameters Used in Simulations 41

Chapter 1

Introduction

This report presents the concluding findings of a three year project concerned with the longitudinal issues regarding modeling and control of vehicles in an Intelligent Vehicles and Highway Systems (IVHS) environment. Specifically, the report addresses the issue of vehicle control in an automated highway system, brake actuation and coordinated throttle and brake control. Recent research findings in the area of automated vehicle platooning on isolated lanes of an automated highway are included. Performance specifications, control system architecture, vehicle control algorithms, actuator and sensor specifications and communication requirements are also addressed. The issue of switching from throttle to brake actuation is addressed in detail.

Chapter 2 deals with the issues of longitudinal vehicle control in an automated highway environment. This chapter looks at the broad concept of Intelligent Transportation Systems (ITS) and how the controls used affect their performance. The idea of "platooning" is analyzed in some detail.

Chapter 3 looks at how the choice of brake actuation strategy essentially fixes the trade-off between passenger comfort and system responsiveness. To simultaneously maintain ride quality and string stability, the system bandwidth must vary inversely with the magnitude of any transport lags in the actuation system.

Chapter 4 discusses the various aspects of brake control development, from actuator design to performance guarantees to experimental validation of the closed-loop system. The subject of actuator design and placement in terms of the brake control issues is also discussed.

Chapter 5 summarizes the results of this report.

Chapter 2

Vehicle Control in Automated Highway Systems

2.1 Introduction

The problems of traffic congestion and safety are becoming more and more critical in almost all metropolitan areas around the world. Many approaches are and have been taken to alleviate this problem including new freeway construction, new public transit facilities, flexible and overlapping working hours, and more recently the use of intelligent transportation systems (ITS). In the broad sense, ITS is the use of modern technological advances to provide increased traffic flow and to reduce traffic accidents. Examples of ITS include sensors that provide flow and incident information to roadway management authorities and to the drivers, computerized traffic lights and freeway ramp metering dependent on current conditions and in-vehicle communication and information displays. More recently there have been research programs in the US (Hedrick *et al.*, 1994; Hedrick, 1995; Shladover and et. al., 1991), Europe (Reichart and Naab, 1994)and Japan to look at various aspects of vehicle automation, ranging from "Intelligent Cruise Control (ICC)" systems that regulate the throttle and possibly the brake to keep a specific distance between the controlled vehicle and the vehicle in front of it, to fully automated highway systems (AHS) where both lateral and longitudinal control is provided automatically. The University of California, PATH program has concentrated on this area of ITS and recently joined with several US industries and universities to form the National Automated Highway System Consortia (NAHSC). This consortia is currently investigating alternative AHS scenarios and will be narrowing down these possibilities after extensive analysis and field testing. This paper will focus on one of these possibilities, the concept of "platooning" or "convoying" where all vehicles are operated under automated vehicle control.

2.2 Performance Specifications

Overall system performance objectives for an automated highway system is outlined in *AHS-System Objectives and Characteristics, Final Draft* (1995). They are stated in terms of improved safety, increased throughput, enhanced mobility and access and reduced environmental impact.

Many potential systems exist that can offer many of the objectives mentioned above. Stevens (1993) outlines many of these possibilities that are currently being thoroughly analyzed by the NAHSC. In this paper only the "platooning" concept will be addressed. Any AHS must offer improved safety characteristics over existing systems. Since most analyses estimate that over 95% of roadway accidents are caused by human driver error, it is reasonable to expect a reduction in accidents with the introduction of automation. *AHS-System Objectives and Characteristics, Final Draft (1995)* sets a goal of 50-80% reduction, depending on the particular AHS system chosen. Figure 2.1 shows the impact velocity of two vehicles as a function of the initial separation before the lead vehicle decelerates. Assumptions have been made (Hedrick, 1995) about deceleration levels, time delays, etc., but the shape of the curve is what is important; i.e., very low impact velocities occur for small initial spacing and for large initial spacing. The platooning approach takes advantage of both ends of Figure 2.1. The vehicles within the platoon are spaced at close separation distances toward the left side of the curve while the platoons are separated from each other at spacing toward the right end of Figure 2.1, thus implying that any collisions that may occur will be low relative velocity impacts.

Clearly one would also hope for an improvement in the capacity or throughput (measured in vehicles/lane/per-hour) over existing systems. Figure 2.2 shows some capacity calculations for various size platoons that satisfy the safety conditions imposed by Figure 2.1. For example, a 15 car

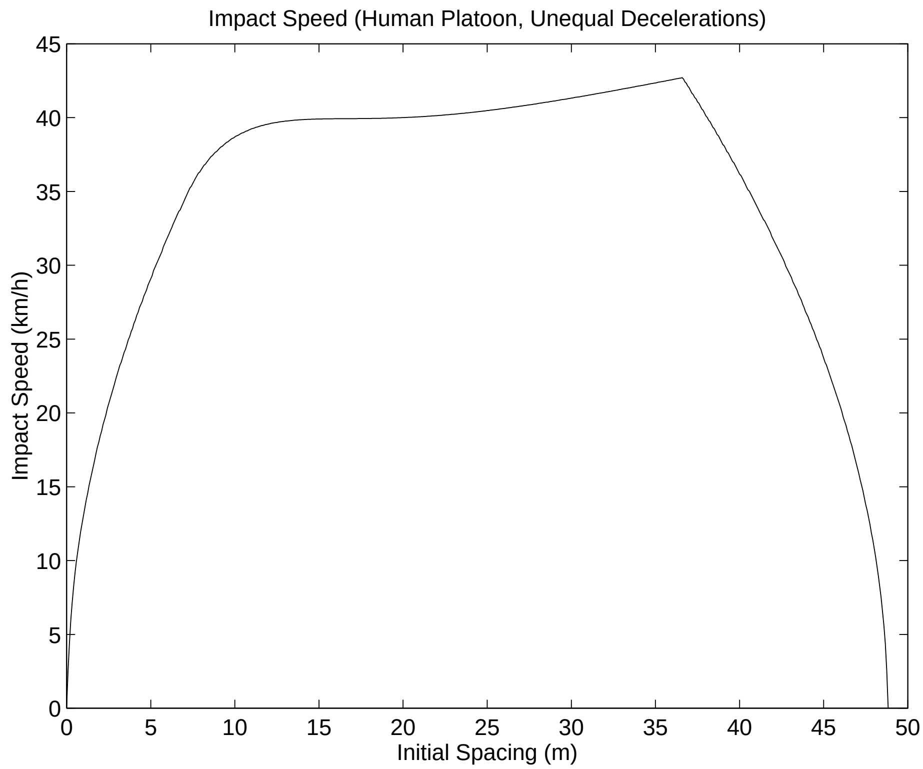

Figure 2.1: Impact Velocity vs. Initial Separation

platoon can offer a three-fold increase in the maximum capacity of existing roads (1995 Highway Capacity Manual) operating in an uncongested state.

The question of the environmental impact of an AHS is currently being studied. It is very clear that the emissions per vehicle kilometer can be greatly reduced since near constant speed operation would automatically achieve this. A more difficult question is the effect on induced demand and the potential that such a system will dramatically increase the total number of kilometers traveled. Current studies within the US NAHSC are addressing this issue.

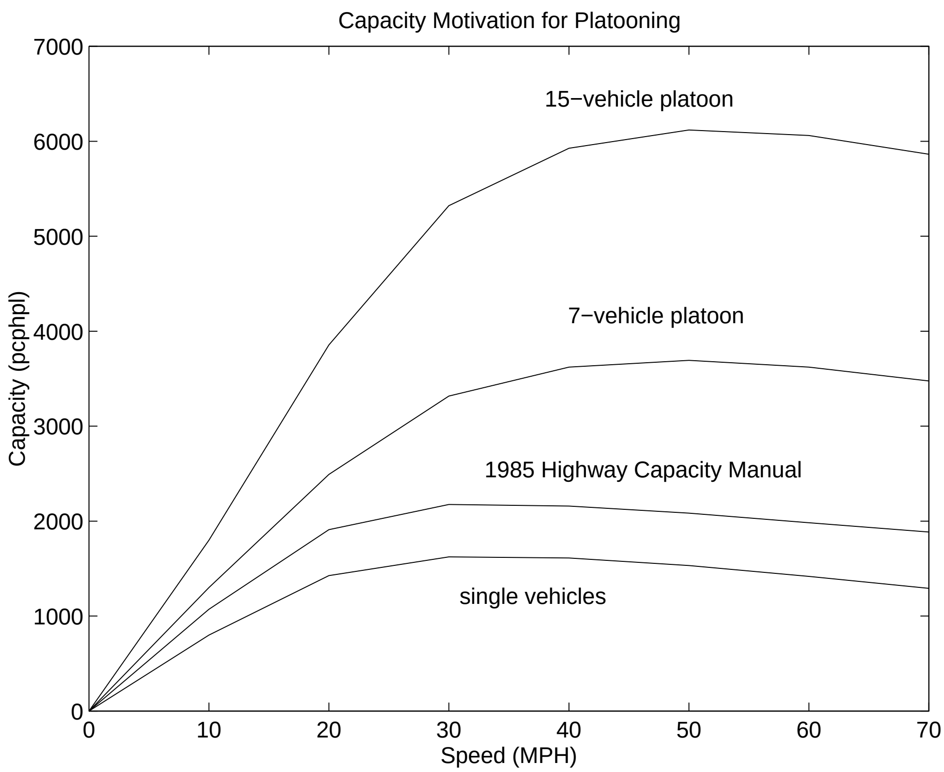

Figure 2.2: Lane Capacity vs. Platoon Size

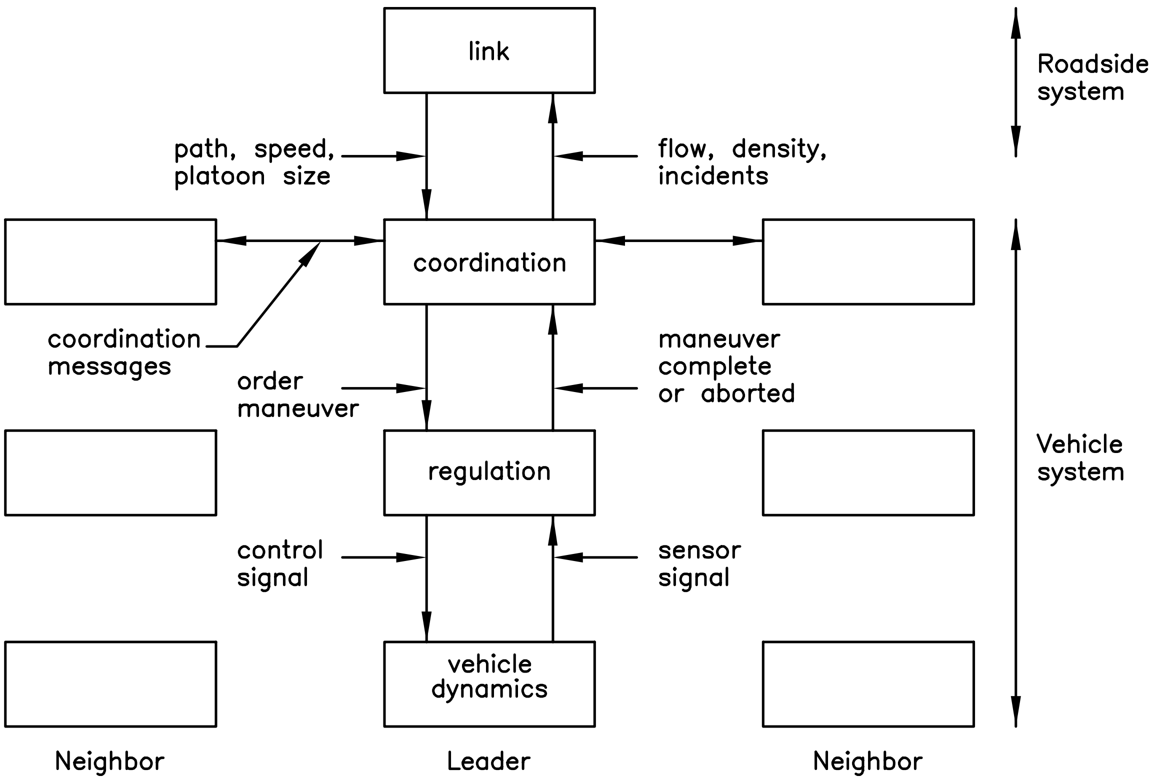

Figure 2.3: PATH Control System Architecture

2.3 Control System Architecture

The basic control system architecture that is currently being considered by PATH (Hedrick *et al.*, 1994; Varaiya, 1993) is shown in Figure 2.3. The architecture must assign a path to each vehicle, carry out maneuvers of platoon formation, stabilization and dissolution, lane change, and entry/exit and to implement these maneuvers with control laws that command each vehicle's throttle, brake and steering actuators. References (Hedrick *et al.*, 1994; Varaiya, 1993) propose a three layer architecture:

1. The top layer is the link layer that broadcasts target values for speed and platoon size based on information about the local speed, density and flow conditions. It will use information about desired exits, detected incidents, etc., to command lane changes, splits and merges.

2. Each vehicle's coordination layer determines which maneuver to initiate at any time so that it will follow the desired path commanded by the link layer. It coordinates this maneuver with neighboring vehicles so that they are accomplished safely. It then commands the next lower layer, the regulation layer, to execute the maneuver. The regulation layer then reports back to the coordination layer that the maneuver has either been completed or aborted. Three maneuvers that are commanded by the coordination layer (Hsu *et al.*, 1993) are: join (two platoons merge into one), split (separates a platoon into two platoons), and lane change (which permits a single car to change lanes).

   Each maneuver requires a communication "protocol," i.e., a structured exchange of messages between relevant neighboring vehicles. A protocol is specified by a set of communicating finite state machines (Hsu *et al.*, 1993).

3. The coordination layer dictates the maneuvers to be performed by the platoon. Each vehicle within the platoon must be able to issue throttle, brake and steering commands to achieve the maneuvers specified by the coordination layer. This is the job of the regulation layer.

Seven feedback laws have been proposed (Hedrick *et al.*, 1994):

1. Lead vehicle velocity tracking. The lead vehicle in the platoon must be able to track the target speed issued by the link layer while also maintaining a safe distance between platoons.
2. Vehicle following. Each vehicle must be able to maintain a close spacing between itself and the preceding vehicle.
3. Join. The lead vehicle accelerates and then decelerates so that two platoons merge.
4. Split. A follower within a platoon decelerates and then becomes the lead vehicle of a new platoon.
5. Lane change
6. Lane entry
7. Lane exit.

2.4 Vehicle Control Algorithms

For non-emergency maneuvers the longitudinal and lateral control functions can be reasonably decoupled and designed separately. These algorithms are described in Hedrick *et al.* (1994), Hedrick (1995), Shladover and et. al. (1991). The longitudinal algorithms have been based on sliding mode control due to the predominantly nonlinear nature of the powertrain dynamics. The lateral algorithms have been based on a linear, frequency shaped LQG approach with gain scheduling on the vehicle's longitudinal velocity. Extensive field testing has shown that these algorithms are capable of excellent performance. References (Tomizuka and Hedrick, 1995; Shladover, 1995) provide an excellent review of AHS control algorithm development.

2.5 Actuator and Sensor Specification

2.5.1 Actuators

Throttle, brake and steering actuators are required for total vehicle automation. Throttle and steering actuators are relatively linear and

range, min/max (m)	.3 to 100 m
range rate, min/max (m/s)	0 to 60
range accuracy	.1 m or 1 % max
range rate accuracy	.1 m/s or 1 % max
update time	10-20 ms
signal processing bandwidth	10 Hz

Table 2.1: Vehicle Range Sensor Specifications

their specifications are straightforward (Hedrick *et al.*, 1994; Hedrick, 1995; Shladover and et. al., 1991; Tomizuka and Hedrick, 1995; Shladover, 1995). Brake dynamics on the other hand are highly nonlinear and inherently different from current ABS actuation systems. Reference (Gerdes and Hedrick, 1995*b*) describes these dynamics and presents brake actuator specifications in terms of an allowable pure time delay (20 ms) and a time constant (.10 seconds). Physically, actuation at the master cylinder is acceptable, provided the system is capable of overcoming seal friction and brake filling without much delay.

2.5.2 Sensors

The area of sensors is perhaps the most important enabling technology for the feasibility of an AHS. A wide variety of sensors are required for the measurement of internal vehicle states (vehicle speed, acceleration, brake pressure, yaw rate, throttle angle, intake manifold pressure), as well as the position of the vehicle with respect to the lane and with respect to neighboring vehicles. There are currently a number of competing alternative technologies. In the area of longitudinal vehicle sensing radar (both microwave and millimeter wave systems), optical systems (laser range finder or LADAR), sonar and vision systems are being evaluated. PATH specifications for a longitudinal sensor for platooning applications (*Ranging Sensors for Use in Longitudinal Control Research*, 1995) are presented in Table 2.1.

The vehicle must also be able to determine its lateral position with respect to the middle of the lane. The primary competing technologies for this application appear to be the magnetic marker system (Peng *et al.*, 1993) currently utilized by PATH and vision systems (Tomizuka and Hedrick, 1995) that have been used in Europe and Japan.

2.6 Communication Requirements

It has been established (Hedrick *et al.*, 1994; Hedrick, 1995; Shladover and et. al., 1991) that closely spaced platooning of vehicles requires vehicle-to-vehicle and roadway-vehicle communication for network performance and safety. It has also been shown (Hedrick and Swaroop, 1993) that vehicle-to-vehicle communications can provide the necessary platoon "damping" to guarantee that inter-vehicle spacing disturbances attenuate as they propagate upstream. There are several applications for communications in an AHS: control, maneuvers and navigation information. In this paper only the control application will be discussed. The current controller update rate for longitudinal control is 20 ms which corresponds to a 50 Hz update rate. Platoon size is uncertain but maximum numbers of 15-20 have been mentioned. This requires a fairly high bandwidth, mostly line-of-sight system with about 1,000 packets/sec. The experimental program at PATH is currently using a WavLAN radio system which uses a direct sequence spread spectrum modulation (Foreman, 1995). A more promising technology for an AHS with many vehicles is the "frequency hopping" spread spectrum modulation. This system has not been tested yet by PATH but is expected to produce excellent results.

2.7 Experimental Results

The PATH program has been involved in experimental verification for many years (Hedrick *et al.*, 1994; Hedrick, 1995; Shladover and et. al., 1991; Choi and Hedrick, 1995). Tests have been conducted on both the magnet based lateral control system (Peng *et al.*, 1993)] and the radar based longitudinal control system (Choi and Hedrick, 1995). The lateral system has achieved accuracies of 10 cm lateral deviation from the centerline while the longitudinal system has operated at 2 m spacing at 90 Kmh with 50 cm deviations.

Chapter 3

Brake Actuation Requirements

3.1 Introduction

As research into Advanced Vehicle Control Systems (AVCS) continues, experimental demonstration of control strategies becomes increasingly important. Moving from theory to test track, however, requires choices in actuation strategy and hardware. For engine control, this choice is fairly intuitive, since the throttle provides a natural control input. Indeed, tight spacing within a platoon of automated vehicles operating under throttle control has been demonstrated both in theory (McMahon *et al.*, 1990) and experiment (McMahon *et al.*, 1992).

In sharp contrast, automotive brake systems (as shown in Figure 3.1) provide no clear actuation point. Because of this, the actuation strategy determines which components remain in the system and, consequently, defines the brake dynamics. A comparable strategy to throttle control (actuating at the pedal) offers an easy retrofit, but incorporates the highly nonlinear dynamics of the vacuum booster in the feedback loop. Bypassing the booster promises enhanced performance, but requires substantial modification to existing brake hardware. Faced with such tradeoffs, the performance requirements of platooning form a critical design parameter.

In this paper, we offer a controls perspective on this issue of performance. Taking the controller framework of McMahon et al., we highlight the critical areas in which the brake system dynamics affect platoon performance. From this, we determine the actuation requirements implicitly specified by the

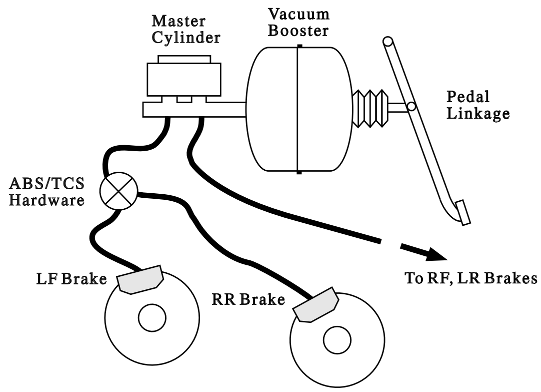

Figure 3.1: Brake System Components

controller structure and robustness demands. Since the maneuvers, tracking accuracy and comfort required by an automated highway are not firmly defined, we adopt a limiting factor approach. By providing some objectives for system design, this paper complements recent results in brake system modeling and control (Gerdes *et al.*, 1995; Gerdes *et al.*, 1993; Maciuca *et al.*, 1994).

We begin by presenting the multiple-surface sliding control scheme for platooning, along with a modified criterion for switching between brake and throttle control. Using this framework, we demonstrate the limitations arising from the vacuum booster cut-in and conclude that an actuation scheme for platooning should bypass this component. Appealing to the dynamics of the two sliding surfaces, we illustrate the need for torque feedback to prevent actuation errors from influencing spacing errors. Finally, we demonstrate how pure time delays in the brake system impose gain limitations that severely hinder the tracking and robustness of the controller. Notes on the feasibility of a such an actuation scheme conclude the paper.

3.2 Vehicle Model and Controller

3.2.1 Throttle Control Development

The analytical basis for this simulation study is a three-state vehicle model (McMahon *et al.*, 1992) where the states are the mass of air in the engine intake manifold, m_a, the engine speed, ω_e, and the brake torque, T_b; the inputs are the throttle angle, α, and the commanded brake pressure, P_{bc}. The state equation for m_a is given by:

$$\dot{m}_a = \dot{m}_{ai} - \dot{m}_{ao} \tag{3.1}$$

where

$$\begin{aligned} \dot{m}_{ai} &= \mathrm{MAX}\,(\mathrm{TC}\,(\alpha))\,\mathrm{PRI}\,(m_a) & (3.2)\\ \dot{m}_{ao} &= c_1 \eta_{vol} m_a \omega_e & (3.3) \end{aligned}$$

In these equations, MAX represents the flow rate at full throttle, TC(α), an empirical throttle characteristic and PRI(m_a) a pressure influence function for compressible flow. η_{vol} is a volumetric efficiency and c_1 a constant based upon engine displacement.

Assuming that the transmission is locked in gear and ignoring tire slip, the state equation for ω_e is:

$$J_e \dot{\omega}_e = T_{net}\,(\omega_e, m_a) - R_g T_b - T_{load} \tag{3.4}$$

where J_e is the vehicle inertia reflected to the engine, T_{net} is the net engine torque and, T_{load}, the drag:

$$T_{load} = C_a {R_g}^3 h^3 {\omega_e}^2 + R_g h F_{rr} \tag{3.5}$$

Here R_g is the gear ratio from engine to wheel, h is the tire radius, C_a the aerodynamic drag coefficient and F_{rr} the total rolling resistance.

The platoon controller is based on the multiple surface sliding control method. Assuming constant desired spacing between vehicles, Δ, we define the spacing error for car i in terms of the position of cars i and $i-1$, x_i and x_{i-1}:

$$\epsilon_i = \Delta - (x_{i-1} - x_i) \tag{3.6}$$

Assuming that lead vehicle information and the car length, L_i, are known, acceptable error dynamics form the first surface (Swaroop and Hedrick, 1994):

$$S_{1i} = \dot{\epsilon}_i + q_1 \epsilon_i + q_3(\dot{x}_i - \dot{x}_{lead}) + q_4(x_i - x_{lead} - \sum_{j=0}^{i} L_i) \tag{3.7}$$

We drive the system to this surface by defining

$$\dot{S}_{1i} = -\lambda_1 S_{1i} \tag{3.8}$$

and solving for $\dot{\omega}_{e,des}$ as a synthetic control:

$$\dot{\omega}_{e,des} = \frac{\ddot{x}_{i-1} - q_1 \dot{\epsilon}_i + q_3 \ddot{x}_{lead} - q_4 \left(\dot{x}_i - \dot{x}_{lead}\right) - \lambda_1 S_{1i}}{\left(1 + q_3\right) R_g h} \tag{3.9}$$

Substituting back into Equation 3.4, we determine a corresponding $T_{net,des}$ and, through table look-up, $m_{a,des}$. Defining the second sliding surface:

$$S_{2i} = m_a - m_{a,des} \tag{3.10}$$

we set

$$\dot{S}_{2i} = -\lambda_2 S_{2i} \tag{3.11}$$

and solve for the desired throttle characteristic:

$$TC_{i,des}\left(\alpha\right) = \left(\dot{m}_{ao} + \dot{m}_{a,des} - \lambda_2 S_{2i}\right) / \left(\text{MAX PRI}\right) \tag{3.12}$$

Inverting this characteristic yields the control, α.

3.2.2 Brake Control Development

In this work, we assume that the actuation system chosen controls the brake pressure at the wheels and possesses a first-order response with transport lag, t_d:

$$\dot{P}_b(t + t_d) = \left(P_{bc}(t) - P_b(t + t_d)\right) / \tau_b \tag{3.13}$$

Within this description, τ_b reflects an effective time constant of the actuator and brake system components and t_d approximates the effects of pure time delays, filling properties, valve spool delays, etc. described in (Gerdes *et al.*, 1995; Gerdes *et al.*, 1993; Ioannou and Xu, 1994). Admittedly, this is a simplification, though sufficient to examine system requirements; more accurate models can be used for implementation. The brake torque is assumed proportional to the pressure through an (uncertain) gain, K_b:

$$T_b = K_b P_b \tag{3.14}$$

If braking is necessary, we substitute Equation 3.9 into Equation 3.4 to determine $T_{b,des}$. Defining:

$$S_{3i} = T_b - T_{b,des} \tag{3.15}$$

and setting

$$\dot{S}_{3i} = -\lambda_3 S_{3i} \tag{3.16}$$

we solve for the input, $P_{bc,des}$, from Equation 3.13:

$$P_{bc} = \left[\tau_b \left(\dot{T}_{b,des} - \lambda_3 S_{3i}\right) + T_b\right] / K_b \tag{3.17}$$

To reflect the difficulty caused by the vacuum booster, one modification is required. Acting as a force amplifier, the booster possesses an internal feedback which moves to command a finite threshold value of braking once triggered. We model this booster "cut-in" by including an additional state:

$$\dot{P}_{vb} = \left(P_{bc,des} - P_{vb}\right) / \tau_{vb} \tag{3.18}$$

with the threshold incorporated as:

$$P_{bc} = \begin{cases} 0 & \qquad\qquad P_{vb} \leq P_{trig} \\ P_{thresh} & P_{trig} < P_{vb} < P_{thresh} \\ P_{vb} & \qquad\qquad P_{vb} \geq P_{thresh} \end{cases} \tag{3.19}$$

For detailed treatment of this component and its other associated control problems, see (Gerdes *et al.*, 1995; Gerdes *et al.*, 1993; Maciuca *et al.*, 1994).

3.2.3 Controller Integration

Because of its roots in engine control, the original controller switched between throttle and brakes depending upon the throttle surface, S_2. In this formulation, switching was based upon the value of α:

$$\begin{array}{lll} \alpha \geq 0 & \Longrightarrow & \text{Throttle} \\ \alpha < 0 & \Longrightarrow & \text{Brake} \end{array} \tag{3.20}$$

Since the switching condition depends upon the gain of the throttle sliding surface, λ_2, problems can arise when switching from brakes to throttle. As demonstrated in Figure 3.2, situations exist where the throttle cuts in before

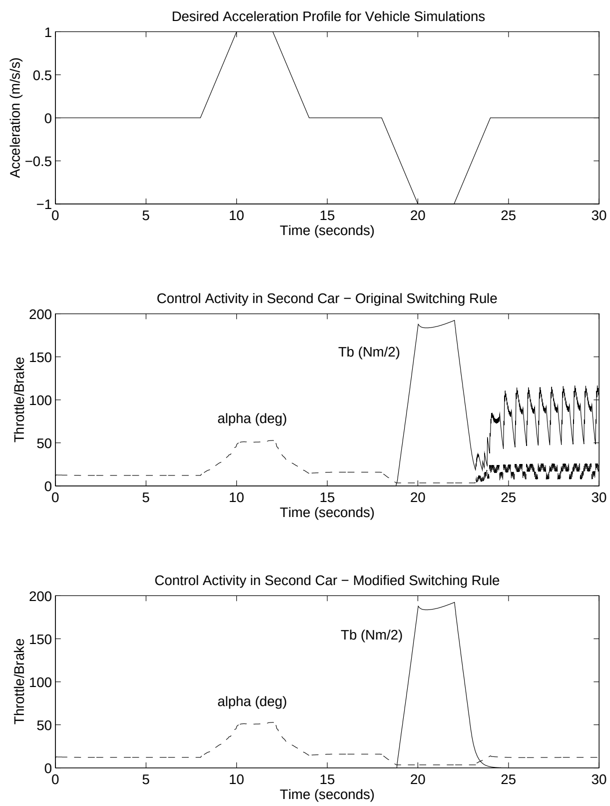

Figure 3.2: Comparison of Switching Rules

the brakes have released sufficiently, resulting in competing control inputs. In previous work (McMahon *et al.*, 1992; McMahon *et al.*, 1990), this problem was eliminated by ignoring the brake torque when using Equation 3.4 to determine $T_{net,des}$. Since braking and robustness to braking torque represent key issues of this paper, we require a more rigorous solution.

We therefore propose a switching strategy where the vehicle enters either throttle or brake control depending upon the level of deceleration commanded. Since rolling resistance and drag provide a certain level of deceleration in the absence of braking, we divide T_{net} into two parts: $T_{e,min}(\omega_e)$ representing the drive torque with no throttle input and T_{ec} denoting the remainder of T_{net}. Then:

$$J_e \dot{\omega}_{e,des} = T_{ec} + T_{e,min} - R_g T_b - T_{load} \tag{3.21}$$

Taking T_b and T_{ec} as our synthetic controls, define

$$T_c = T_{ec} + R_g T_b \tag{3.22}$$

Substituting into Equation 3.21, we get

$$T_{c,des} = J_e \dot{\omega}_{e,des} + T_{load} - T_{e,min} \tag{3.23}$$

A positive value of $T_{c,des}$ therefore requires throttle control and a negative value results in braking. Since T_{load} and $T_{e,min}$ are functions of engine speed, switching becomes a function of ω_e and $\dot{\omega}_{e,des}$ alone. Removing the dependence on λ_3 results in well-defined periods of throttle control and braking (Figure 3.2).

3.3 Simulation Results

3.3.1 Methodology

Numerical simulations involving platoons of 10 and 20 vehicles following the maneuver depicted in Figure 3.2 were performed using the simulation code described in (McMahon *et al.*, 1992). The vehicle parameters correspond to the Lincoln Town Cars used as experimental vehicles by the California PATH Program and may be found in (McMahon *et al.*, 1990). As noted in the Introduction, a limiting factor approach was taken. The results and implications that follow, therefore, are based upon the premise that platoon performance should not be hindered by that of the brake system. The vehicle parameters correspond to the Lincoln Town Cars used as experimental vehicles by the California PATH Program and may be found in (McMahon *et al.*, 1990). The specific brake and control constants used for this study, except where noted were: λ_1=1, λ_2=40, λ_3=25, q_1=1, q_2=1, q_4=0.5, τ_b=0.10s, τ_{vb}=0.010s, K_b=1.11 Nm/kPa, P_{thresh}=300 Nm, P_{trig}=0.5 Nm.

3.3.2 Vacuum Booster

As Figure 3.2 shows, the braking required by the standard simulation maneuver is gradual and of low amplitude. This contrasts sharply with human brake commands and, consequently, the vacuum booster cut-in. Intuitively, there are two methods for reconciling this: modulate the input in an attempt to achieve lower values of brake torque or actuate the brakes only after this threshold level of deceleration is commanded. Figure 3.3 demonstrates the difficulties caused by modulation. The rapid changes in the brake torque cause passenger comfort to suffer from increased jerk while tracking of the desired torque and spacing also deteriorates. Admittedly, this is more illustration than proof, since the booster remains uncompensated in the control law. However, more sophisticated control efforts have produced similar results in theory and experiment (Maciuca *et al.*, 1994). The amplitude and frequency of modulation changes with actuator and control choice, but the basic problem persists.

A possible solution, then, is to emulate a human driver and switch to braking only after the threshold corresponding to booster cut-in is commanded. Assuming that the large jerk upon application is smoothed (similar to the acceleration limit in (Ioannou and Xu, 1994)), ride quality may be achieved. Spacing, as illustrated in Figure 3.4, however, suffers. Such effects are even more noticeable when levels of deceleration below the cut-in threshold are commanded and when lead vehicle position is not available (q_4=0).

These spacing errors arise because the sliding surface dynamics in Equation 3.7 assume that $T_{c,des}$ is tracked accurately. Since the dynamics of this upper surface must provide ride quality (and control activity translates to acceleration and jerk), they are too slow to compensate for actuation errors. As a result, braking errors propagate to spacing errors. This need for tight

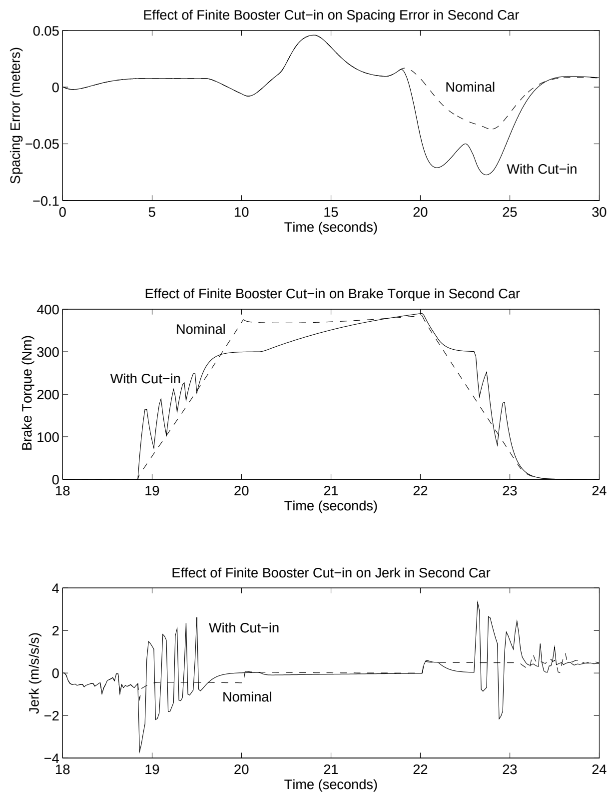

Figure 3.3: Effects of Booster Cut-in Force

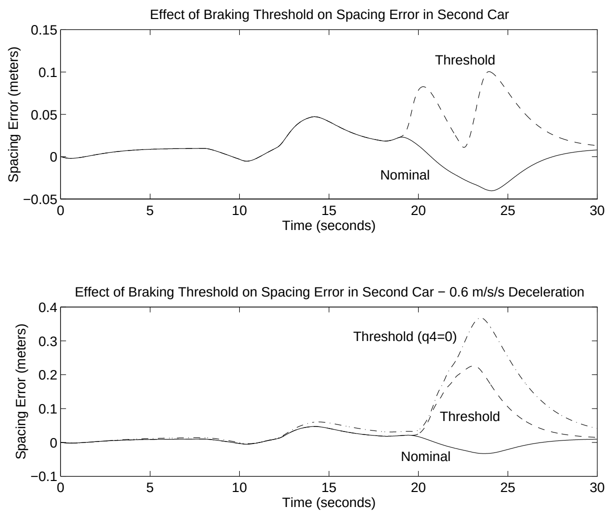

Figure 3.4: Effects of Braking With Threshold

tracking of brake torque is the key to defining performance requirements.

3.3.3 Torque Feedback

Because of the problems with the cut-in, bypassing the booster clearly represents a more appealing strategy than modulating or thresholding. In practice, this bypass may be achieved either by inserting an actuator between the booster and master cylinder or by modulating the brake pressure directly (perhaps through a Traction Control System). Since either approach entails substitution of actuator dynamics for brake dynamics, some notion of the desired characteristics of such a system is required for design. We begin with the question of feedback.

Since the gain K_b can vary up to 40% due to temperature effects alone (Radlinski, 1991), controlling brake pressure is not equivalent to controlling the torque. Furthermore, the upper surface provides little correction for actuation errors, so potential mismatch in this gain must be compensated by the brake controller. Figure 3.5 compares nominal controller performance with performance when the controller underestimates K_b by 30%, assuming feedback of either T_b or P_b. With torque feedback, the gain is countered by the robustness term in the brake surface, with tracking comparable to the

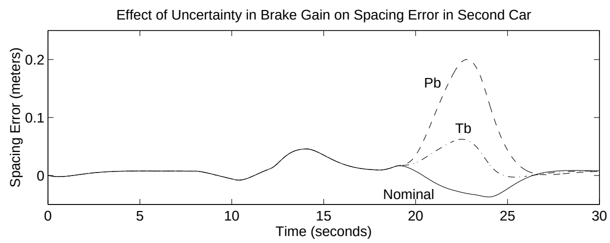

Figure 3.5: Performance With Brake Gain Mismatch

nominal case; with pressure feedback, large spacing errors occur. As with the threshold, setting q_4=0 produces even larger disturbances.

While the need for feedback is clear, the method is not as obvious. Although brake torque has been extracted from accelerometer measurements for analysis purposes (Gerdes *et al.*, 1995; Gerdes *et al.*, 1993), the presence of suspension modes and other vibrations in the data presents a serious obstacle for measuring low torques. Direct measurement (Hurtig *et al.*, 1994; Perronne *et al.*, 1994) appears to be a more promising solution, and represents a current research area.

3.3.4 Actuator Dynamics

Having established the booster limitations and the need for feedback, we turn to the desired dynamic response of a brake system. In the context of the brake model assumed in Equation 3.13, the time constant τ_b represents the least stringent requirement. Ideally, this value is cancelled by the control law in Equation 3.17. Practically, saturation becomes an issue, though the smooth variation in the desired brake torque results in reasonable control inputs for τ_b in the range of 0.10 to 0.20 (the stock brake hydraulics possess a time constant on the order of 0.08-0.10 seconds).

The time delay, however, represents a more serious problem. Because of the relatively large gain on the surface S_3, delays result in oscillatory braking commands, hindering both tracking and comfort. Figure 3.6 contrasts the performance of the system without delay to that with an 80 millisecond delay. Since the effects of this delay increase down the platoon (due to dependence on previous vehicle information), this case shows a loss of string stability by the 8th car. Furthermore, the comfort level (measured by the

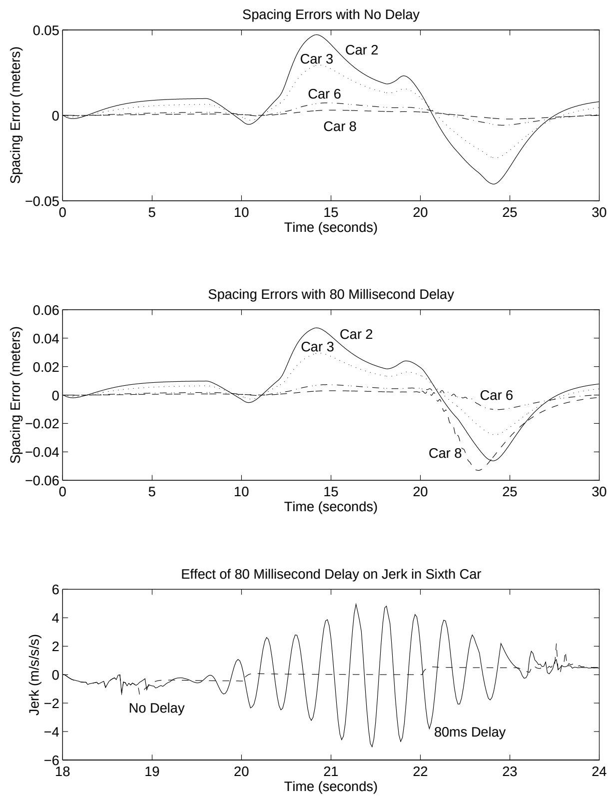

Figure 3.6: Effects of 80 Millisecond Delay

jerk) deteriorates rapidly down the platoon.

Such problems can be eliminated by either reducing the sliding gain, λ_3, or boosting the time constant, τ_b. Boosting the time constant, however, requires actuating downstream of the master cylinder with an extremely fast actuator. While possible, this presents a serious design task. Reducing the sliding gain is much easier, but produces a decrease in performance. As illustrated in Figure 3.7, spacing errors increase slightly when this gain is reduced, but robustness to the brake gain error of Section 3.3.3 decreases noticeably.

A number of simulations similar to those above were conducted to quantify acceptable levels of delay. From these results, we conclude that a brake system with a time constant of 0.10 seconds and delay time of 20 milliseconds requires no reduction in λ_3 from the ideal case and exhibits no

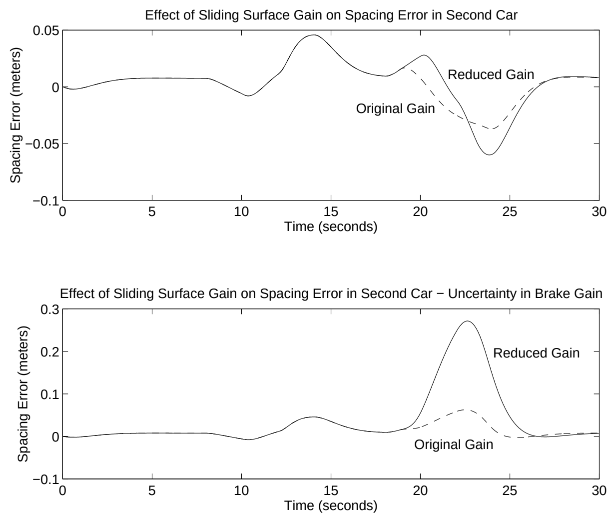

Figure 3.7: Effect of Sliding Gain on Spacing Errors

noticeable decrease in comfort or tracking for a 20 car platoon. Physically, this implies that actuation at the master cylinder is acceptable, provided the system is capable of overcoming seal friction and brake filling (Gerdes *et al.*, 1995) without much delay.

Chapter 4

Brake Control Development

This chapter discusses the various aspects of brake control development, from actuator design to performance guarantees to experimental validation of the closed-loop system. Section 4.1 treats the subject of actuator design and placement in terms of the brake control issues presented in the previous chapter. Implementation of the solution chosen for this work - a separate hydraulic system with an actuator mounted in series between the vacuum booster and master cylinder - is considered and this method compared to modulation of an Anti-Lock Braking System (ABS) or Traction Control System (TCS). Section 4.2 takes the hydraulic state equation of the previous chapter and develops a sliding controller capable of fast, accurate pressure control. To avoid problems in implementation, however, modification of the basic structure is required. Section 4.3 presents a rigorous treatment of the controller behavior with this modification and proves that the resulting control scheme is stable, exhibits an exponential decay of tracking error after a finite time and displays robustness to parametric uncertainty. Section 4.4 briefly discusses the introduction of a saturation function in this structure in order to reduce the potentially high initial control activity. Simulation results of the closed-loop braking system are presented in Section 4.5 and the chapter concludes with experimental tracking results.

4.1 Actuator Design

As the previous chapter demonstrated, the brake vacuum booster possesses several characteristics that serve to limit controller performance severely. Consequently, a brake actuation design that bypasses the booster can reasonably be expected to exhibit higher performance and rely more heavily on the dynamics of the hydraulic system. This reliance is an asset to the control designer since, the model of the brake hydraulics is indeed quite accurate.

Two methods of accomplishing such actuation are immediately apparent: modulate the action of an Anti-Lock Braking System (ABS) or Traction Control System (TCS) capable of brake application (some ABS systems only *release* pressure) or develop a method of applying force to the master cylinder directly. The former is without question a more realistic approach to the design of hardware intended to be implemented in an actual production vehicle. However, this requires fairly heavy modification of proprietary hardware and, therefore, the risk of compromising vehicle safety systems. As a result, the latter method was used to produce an experimental system for these investigations.

The system design - shown in Figure 4.1 - creates a separate hydraulic circuit for brake actuation with the addition of a single-acting cylinder in series between the booster and master cylinder. Power is obtained from a hydraulic accumulator charged by flow from a second power steering pump attached to the accessory belt. The actuator pressure is modulated by a Vickers SM4 servovalve, which can alternately attach the cylinder to either the accumulator pressure or the atmospheric pressure of the tank. This particular hydraulic circuit was chosen so that an automated brake application would never exert force in opposition to the driver's braking (as in the case of a double-acting cylinder upon release). As a result, the driver can always produce braking above that requested by the system or, by hitting a switch on the dash, remove power to the system and cause the fluid to drain into the tank. This feature, in addition to the design and construction of the hydraulic supply system and actuator cylinder, is due to Pete Devlin of the California PATH Program.

Since the servovalve, in an open loop sense, controls flow, some feedback is necessary to produce a pressure control loop. This feedback - alternately chosen to be the pressure in the brake system just after the master cylinder

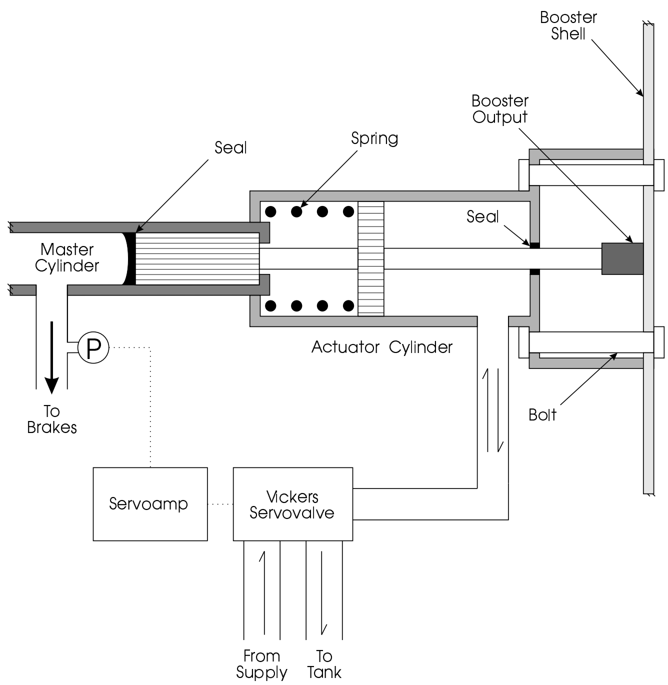

Figure 4.1: Direct Master Cylinder Actuation System

and the pressure in the actuator cylinder - is incorporated into a simple analog proportional controller for the valve. Because of its placement near the valve (and not in the cylinder itself), the actuator pressure signal possessed considerable noise due to pressure transients. As a result, the master cylinder pressure signal produced a cleaner feedback signal and allowed for a higher control gain. The only difficulty with using this measurement was that some error arose due to the inclusion of the spring force and master cylinder seal friction in the control loop. This error was not terribly large, so the master cylinder pressure feedback was chosen for the experimental system.

While this approach is quite different than modulating an ABS or TCS circuit, the idea of controlling a pressure upstream of the caliper is the same. As a result, the dynamic equations governing the brake hydraulics are also quite similar. Therefore, the control scheme presented and analyzed in this chapter should be implementable on ABS or TCS hardware as well, with merely a change of parameters and the possible inclusion of actuator dynamics. Further evidence of this assertion can be found in the brief discussion of brake modeling for ABS and TCS contained in van Zanten *et al.* (1995).

4.2 Sliding Controller Design

With the actuation scheme described in the previous section (and a sufficiently fast hydraulic valve), we can take the pressure in the master cylinder to be our control input to the brake system. The system dynamics are thus defined by the brake hydraulics:

$$\tau_b = \begin{cases} K_b(P_w - P_{po}) & P_w > P_{po} \\ 0 & \text{otherwise} \end{cases} \tag{4.1}$$

$$P_w = P_w(V) \tag{4.2}$$

and

$$\dot{V} = \sigma C_q \sqrt{|P_{mc} - P_w|} \tag{4.3}$$

where $\sigma = sgn(P_{mc} - P_w)$. The relationships upon which Equations 4.1 and 4.2 are based are shown in Figures 4.2 and 4.3, respectively. This controller was implemented on a different car than that used for modeling

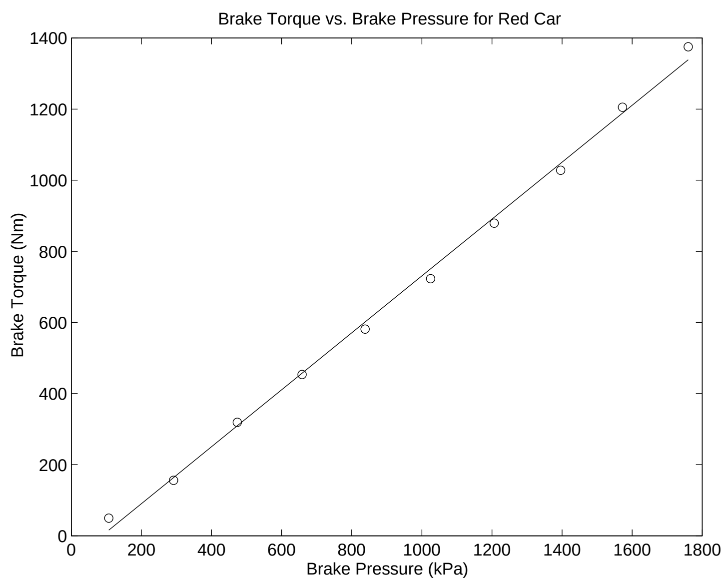

Figure 4.2: Experimental Data for Brake Torque vs. Brake Pressure

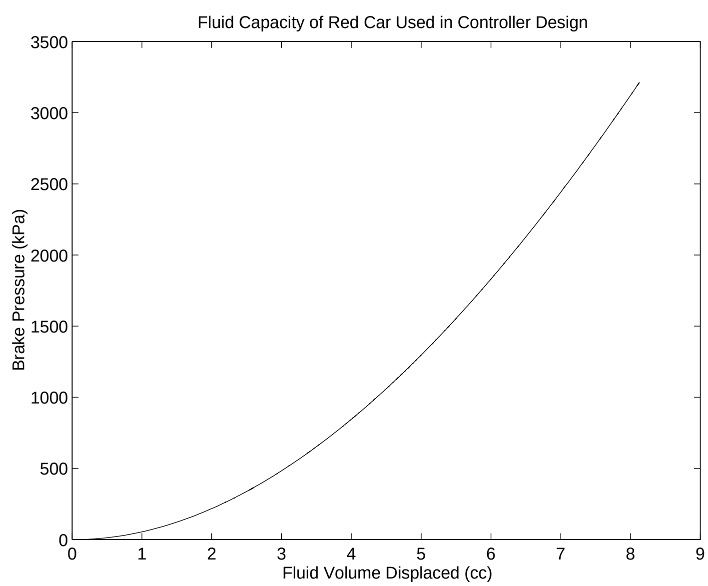

Figure 4.3: Brake Fluid Capacity Curve Used for Controller Design

(although the same year and model), accounting for the slight variations in these relationships.

The simplest control scheme for the brake system, of course, is to send out a desired pressure command to the actuator and simply ignore the brake line dynamics. Such a strategy seems suboptimal since it would clearly introduce undesired lag between the actual and desired brake pressures. There is an even greater reason not to take this approach, however. During general maneuvers in a platoon, the brake pressures required are generally rather small; hence the flow rate, $\dot{V}$, resulting from these open loop commands is also quite small. Because of the nature of the fluid capacity curve in Figure 4.3, the system therefore exhibits long delays between the time the brake pressure is commanded and the time that sufficient fluid has been displaced to create a pressure at the wheel. These delays in braking can exacerbate switching problems between brake and throttle control and, as noted by Gerdes and Hedrick (1995a), lead to performance constraints on the automated vehicle. Some form of lead compensation, therefore, is clearly required.

Before presenting a specific controller design capable of achieving this compensation, the question of feedback should be addressed. In the results that follow, we assume that feedback comes from the wheel pressure, so that the control objective is for P_w to track some desired profile, $P_{wdes}(t)$. One reason for this is that feedback of the volume requires measurement of the actuator stroke, which is not available on the present system. Even if it were, tracking a desired volume would not enclose the function $P_w(V)$ in the feedback loop, so errors in this function would result in errors in braking. Following this line of thought, the brake torque would be the ideal feedback, since it would also include the uncertain gain, K_b, in the control loop. Unfortunately, sensors capable of this measurement are prohibitively expensive and often have trouble measuring accurately at low torques. While low-cost torque measurement techniques are an active area of research (Hurtig *et al.*, 1994; Perronne *et al.*, 1994), pressure feedback currently represents the most realistic solution.

Since the plant dynamics therefore describe a first-order, nonlinear system, we choose the nonlinear design technique of sliding control. Discussion of this technique can be found in Slotine and Li (1991), though the development here is quite straightforward and requires little background.

Using the terminology of sliding control, define an error surface to be:

$$S_b = P_{wdes} - P_w \tag{4.4}$$

and set the desired dynamics of this error to be

$$\dot{S}_b = -\lambda_b S_b \tag{4.5}$$

Substituting the actual dynamics yields

$$\dot{P}_w = \dot{P}_{wdes} - \lambda_b S_b \tag{4.6}$$

where

$$\dot{P}_w = \frac{\partial P_w}{\partial V} \sigma C_q \sqrt{|P_{mc} - P_w|} \tag{4.7}$$

If Equation 4.7 were well-defined everywhere, it could be used in conjunction with Equation 4.6 to determine the desired value of the control input, P_{mc}. Unfortunately, because of the nature of the wheel capacitance in Figure 4.3, $\frac{\partial P_w}{\partial V}$ is not defined until the initial flow to the caliper occurs. Hence, a strict application of such a control strategy makes no sense. If, however, the value of $\frac{\partial P_w}{\partial V}$ is limited in the controller, this problem can be resolved.

Under such a scheme, define a lower limit on $\frac{\partial P_w}{\partial V}$ in the controller to be a and the pressure and volume at which $\frac{\partial P_w}{\partial V} = a$ to be P_a and V_a. Then the master cylinder pressure commanded can be given by the following structure:

$$\dot{P}_{wdes} > \lambda_b(P_w - P_{wdes}) \quad \rightarrow \quad P_{mc} = P_w + \left(\frac{\dot{P}_{wdes} - \lambda_b\left(P_w - P_{wdes}\right)}{\frac{\delta P_w}{\delta V} C_q} \right)^2 \tag{4.8}$$

$$\dot{P}_{wdes} < \lambda_b(P_w - P_{wdes}) \quad \rightarrow \quad P_{mc} = P_w - \left(\frac{\dot{P}_{wdes} - \lambda_b\left(P_w - P_{wdes}\right)}{\frac{\delta P_w}{\delta V} C_q} \right)^2 \tag{4.9}$$

where

$$\frac{\delta P_w}{\delta V} = \begin{cases} \frac{\partial P_w}{\partial V} & P_w > P_a \\ a & \text{otherwise} \end{cases} \tag{4.10}$$

Note that since we are taking P_w as the feedback, this involves writing $\frac{\delta P_w}{\delta V}$ as a function of P_w and not V; justification for this is presented in the next section. In practice, P_a can be chosen to be below the pushout pressure, P_{po}, at which braking commences. Loosely speaking, therefore, we are only interested in pressures above P_a and the controller functions as a sliding controller above P_a. Hence, the modified controller should provide tracking exactly as a sliding controller in our region of interest. This intuitive feeling about the controller performance will be made rigorous in the next section.

Within the context of braking control for an automated highway, one other modification should be noted. Since the vehicle control will consist of alternate periods of throttle control and brake control, a switch from throttle (with $P_{wdes} = 0$) to brake control at $t = 0$ entails a switch from $P_{wdes}(0^-) = 0$ to $P_{wdes}(0^+) = P(0) \geq P_{po}$. As a result, the $\dot{P}_{wdes}$ term in the above equations is somewhat ambiguous. This difficulty is handled by assuming that $P_{wdes}(0^-) = P(0)$ in the controller; in other words, allowing the controller to "see" the initial tracking error, but not attempting to track a discontinuous trajectory. This modification is assumed in the performance guarantees that follow.

4.3 Performance Guarantees

The controller structure presented above is relatively simple, but requires a modification to account for the initial flatness of the fluid capacity curve. Furthermore, uncertainties can arise in the model, particularly with regards to caliper knockback. While intuition suggests such issues to be minor, the exact controller behavior in the presence of all of these factors is not immediately obvious. By exploiting the first-order linear dynamics of the sliding controller, however, performance guarantees can be made in a very straightforward manner.

Before making any statements regarding the controller performance, however, we begin with an assumption on the class of brake pressure trajectories we intend to track:

Assumption 1 (Desired Brake Pressure Profile) *The desired brake pressure profile, $P_{wdes}(t)$, satisfies the following criteria:*

1. *$P_{wdes}(t)$ is defined and differentiable on some interval* $[0, t_f]$.
2. $P_{wdes}(t) \geq P_{po} > P_a \quad \forall t \in [0, t_f]$
3. $P_{wdes}(0) \leq \bar{P}(0)$
4. $\dot{P}_{wdes}(t) \leq \bar{\dot{P}}_{wdes} \quad \forall t \in [0, t_f]$

The first criterion merely ensures that the controller design (incorporating $\dot{P}_{wdes}$) is well-defined. The closed interval $[0, t_f]$ is used to reflect the fact that finite periods of braking exist; the mathematics hold, however, for trajectories defined on $[0, \infty]$. The second and third are related to physical constraints of the problem. Clearly, if the desired pressure is less than the push-out pressure, no braking occurs and the trajectory is meaningless as a brake trajectory. Similarly, we choose $P_a < P_{po}$ so that the controller will function as desired for all $P_{wdes} > P_{po}$. The constraint on the initial value of P_{wdes} is a fairly loose, implying only that this value is bounded. This presents a very mild assumption on the throttle/brake switching logic which holds, in particular, for the switching control developed in the next chapter.

The constraint on the magnitude of $\dot{P}_{wdes}$ is only needed later, when uncertainty is considered. Having some bound on this value allows us to bound the tracking error in the event of uncertainty. Clearly, if discontinuous changes in P_{wdes} are allowed, time domain tracking bounds are meaningless. This also applies to sliding controllers with gain uncertainty following a trajectory which possesses an unbounded, continuous derivative.

In addition to the trajectory, the other factors involved in this analysis are the fluid capacity curve of Figure 4.3 and the flow coefficient, C_q. Physically, these factors must satisfy certain constraints due to the nature of brake systems. This physical intuition is captured mathematically by the following assumption:

Assumption 2 (Brake System Properties) *The flow coefficient, C_q, satisfies $C_q > 0$. The brake fluid capacity curve, $P_w(V)$, satisfies*

1. $P_w(V) = 0 \qquad \forall\, V \leq V_o$
2. $P_w(V) > 0 \qquad \forall\, V > V_o$

for some volume V_o. Furthermore, for $V > V_o$, $P_w(V)$ is a strictly increasing, differentiable function of the displaced volume, V, i.e.

$$\frac{\partial P_w}{\partial V} > 0 \quad \forall\, V > V_o$$

Because of this assumption, we can think of $P_w(V)$ as a function, $P_w(V - V_o)$, defined for $V \geq V_o$, and a shift along the V axis, denoted by V_o. Such an interpretation is particularly useful for dealing with the model uncertainties discussed in Section 4.3.2. Additionally, since $\frac{\partial P_w}{\partial V} \neq 0$ for $V > V_o$, we can define an inverse function P^{-1} such that $V - V_o = P^{-1}(P_w)$ and write

$$\frac{\partial P_w}{\partial V}(V - V_o) = \frac{\partial P_w}{\partial V}\left(P^{-1}(P_w)\right) \tag{4.11}$$

Thus we can (with only slight abuse of notation) write $\frac{\partial P_w}{\partial V}(P_w)$, which enables us to implement the control structure of Equations 4.8 through 4.10 without measuring the volume.

4.3.1 Error Dynamics

With the physics of the system now properly characterized by mathematics, the system performance may be examined rigorously. We begin with the dynamics of the tracking error when the system model is assumed known.

Proposition 1 (Error Dynamics)
Under the control structure in Equations 4.8 through 4.10 with P_a chosen such that

$$P_a < P_{po}$$

if the desired pressure profile satisfies Assumption 1 and the brake system satisfies Assumption 2, the tracking error begins an exponential decay after a finite time, t_s.

Proof To see this, consider the state equation for brake fluid volume while the wheel pressure, P_w, is below P_a (i.e. $V \leq V_a$):

$$\dot{V} = \frac{1}{a}\left[\dot{P}_{wdes} - \lambda_b\left(P_w - P_{wdes}\right)\right] \tag{4.12}$$

when $P_w = 0$ ($V \leq V_o$), this simplifies to:

$$\dot{V} = \frac{1}{a}\left[\dot{P}_{wdes} + \lambda_b P_{wdes}\right] \tag{4.13}$$

There are thus three stages of operation for the controller: when $P_w = 0$, when $0 < P_w \leq P_a$ and when $P_w \geq P_a$. In this final stage, the dynamics satisfy Equation 4.5 and, hence, exhibit exponential error convergence. The proof of this proposition, therefore, involves showing that the system will reach P_a in a finite time for any admissible desired trajectory.

Before enough fluid flows into the caliper to produce a brake pressure rise, the fluid evolution is given by integrating Equation 4.13:

$$V(t) = \frac{1}{a}\int_0^t \dot{P}_{wdes} dt + \frac{\lambda_b}{a}\int_0^t P_{wdes} dt \tag{4.14}$$

Denoting the time at which $V = V_o$ by t_1:

$$V(t_1) \doteq V_o = \frac{1}{a}\int_0^{t_1} \dot{P}_{wdes} dt + \frac{\lambda_b}{a}\int_0^{t_1} P_{wdes} dt \tag{4.15}$$

From Assumption 1, we can determine minimum values for the two terms above, namely

$$\int_0^{t_1} \dot{P}_{wdes} dt \geq P_{po} - \bar{P}(0) \tag{4.16}$$

and

$$\int_0^{t_1} P_{wdes} dt \geq P_{po} t_1 \tag{4.17}$$

so that

$$V_o \geq \frac{1}{a}\left[P_{po} - \bar{P}(0)\right] + \frac{\lambda_b}{a} P_{po} t_1 \tag{4.18}$$

and

$$t_1 \leq \frac{V_o a + \left[\bar{P}(0) - P_{po}\right]}{\lambda_b P_{po}} \doteq \bar{t}_1 \tag{4.19}$$

Similarly, using Equation 4.12, and defining t_2 to be the time at which $V = V_a$:

$$V(t_2) \doteq V_a = V_o + \frac{1}{a}\int_{t_1}^{t_2} \dot{P}_{wdes} dt + \frac{\lambda_b}{a}\int_{t_1}^{t_2} (P_{wdes} - P_w) dt \tag{4.20}$$

Again, using Assumption 1 and the fact that $P_w \leq P_a$,

$$V_a \geq V_o + \frac{1}{a}\left[P_{po} - \bar{P}(0)\right] + \frac{\lambda_b}{a}(P_{po} - P_a)(t_2 - t_1) \tag{4.21}$$

This introduces some conservativism, but illustrates that

$$t_2 \leq \bar{t}_1 + \frac{(V_a - V_o)a + \left[\bar{P}(0) - P_{po}\right]}{\lambda_b(P_{po} - P_a)} \qquad (4.22)$$

Thus, for any admissible trajectory, the volume will equal V_a in finite time, $t_s = t_2$, after which the dynamics satisfy the exponential decay with rate λ_b defined by Equation 4.5. □

4.3.2 Robustness

There are, of course, limitations as to how accurately the brake system can be modeled, leading to parametric uncertainties in C_q, V_o and the fluid capacity curve $P_w(V)$. Of these values, V_o is particularly subject to variation as a result of caliper knockback. During driving, the various vehicle vibrations cause the brake calipers to be "knocked back" arbitrary distances from the discs. This behavior results in a fluid capacity curve that is shifted along the volume axis or, analogously, an error in V_o. The above proposition, however, can be generalized for this uncertain case.

First, we make some assumptions regarding bounds on the modeling error.

Assumption 3 *Given actual parameter values, V_o, C_q and $P_w(V - V_o)$, and the corresponding modeled values, V_{om}, C_{qm} and $P_{wm}(V - V_{om})$, where the modeled values also satisfy Assumption 2, define P_{am}, V_{am}, and V_a such that*

$$\begin{aligned} \frac{\partial P_{wm}}{\partial V}(P_{am}) &= a \\ P_{wm}(V_{am}) &= P_{am} \\ P_w(V_a) &= P_{am} \end{aligned}$$

The discrepancies between the system and model should therefore satisfy the following:

1. $|V_o - V_{om}| \leq \tilde{V}_o$
2. $|V_a - V_{am}| \leq \tilde{V}_a$
3. $\beta_C^{-1} \leq \frac{C_q}{C_{qm}} \leq \beta_C$

4. $\beta_{PV}^{-1} \leq \frac{\frac{\partial P_w}{\partial V}(P_w)}{\frac{\partial P_{wm}}{\partial V}(P_w)} \leq \beta_{PV} \quad \forall P_w \geq P_{am}$

for some $\tilde{V}_o$*,* $\tilde{P}_a$*,* β_C *and* $\beta_{PV} \in \Re$ *with* $\beta_C, \beta_{PV} > 1$*.*

The bounds in (3) and (4) above are stated in terms of the ratio between actual and modeled parameters merely for the sake of notation. As noted in Slotine and Li (1991), bounds on some variable α of the form $0 < \alpha_{min} \leq \alpha \leq \alpha_{max}$ can easily be translated into bound of the form above on the ratio $\frac{\alpha}{\alpha_m}$. Note that uncertainty in the the slope of the fluid capacity curve is only specified above a certain level of pressure; below this level, any amount of uncertainty is allowable (subject of course to Assumption 2). This property is extremely practical, since concrete statements about the slope at very low pressures are nearly impossible to make from experimental data.

With this class of uncertainties, the system performance remains relatively unchanged, although perfect tracking is no longer possible:

Proposition 2 (Robustness of Error Dynamics) *Under Assumptions 1 and 2 and the controller structure given by Equations 4.8 to 4.10, with* P_{am} *chosen to satisfy*

$$P_{am} < P_{po}$$

the tracking error begins an exponential decay to a boundary layer around zero in finite time even in the presence of parametric uncertainties satisfying Assumption 3.

Proof The proof is similar to that of Proposition 1, in that the first task is to show that under any admissible trajectory, the pressure will reach P_{am} in finite time. Note that for $P_w \leq P_{am}$, the state equation for brake fluid volume satisfies a relationship analogous to Equation 4.12:

$$\dot{V} = \frac{C_q}{C_{qm}} \frac{1}{a} \left[\dot{P}_{wdes} - \lambda_b (P_w - P_{wdes}) \right] \tag{4.23}$$

Thus the time bounds in Equations 4.19 and 4.22 may be computed in a similar manner. Rewriting in terms of the model parameters and bounds, this gives

$$t_1 \leq \frac{(V_{om} + \tilde{V}_o)\beta_C a + \left[\bar{P}(0) - P_{po} \right]}{\lambda_b P_{po}} \doteq \bar{t}_1 \tag{4.24}$$

$$t_2 \leq \bar{t}_1 + \frac{(V_{am} - V_{om} + \tilde{V}_a + \tilde{V}_o)\beta_C a + \left[\bar{P}(0) - P_{po}\right]}{\lambda_b (P_{po} - P_{am})} \tag{4.25}$$

so the system reaches P_{am} in finite time.

At this point, the master cylinder pressure is chosen according to

$$\sigma \sqrt{|P_{mc} - P_w|} = \frac{\dot{P}_{wdes} - \lambda_b (P_w - P_{wdes})}{\frac{\partial P_{wm}}{\partial V} C_{qm}} \tag{4.26}$$

and the actual pressure dynamics satisfy

$$\dot{P}_w = \frac{\frac{\partial P_w}{\partial V}}{\frac{\partial P_{wm}}{\partial V}} \frac{C_q}{C_{qm}} \left[\dot{P}_{wdes} - \lambda_b (P_w - P_{wdes})\right] \tag{4.27}$$

This, in turn, produces error dynamics given by

$$\dot{S}_b = -\left(\frac{\frac{\partial P_w}{\partial V}}{\frac{\partial P_{wm}}{\partial V}} \frac{C_q}{C_{qm}}\right) \lambda_b S_b + \left(\frac{\frac{\partial P_w}{\partial V}}{\frac{\partial P_{wm}}{\partial V}} \frac{C_q}{C_{qm}} - 1\right) \dot{P}_{wdes} \tag{4.28}$$

These dynamics represent an exponential convergence with rate λ where

$$\beta_C^{-1} \beta_{PV}^{-1} \lambda_b \leq \lambda \leq \beta_C \beta_{PV} \lambda_b \tag{4.29}$$

to a boundary layer $|S_b| \leq \Phi$ with

$$\Phi \leq \frac{(\beta_C \beta_{PV} - 1)}{\lambda_b} \dot{\bar{P}}_{wdes} \tag{4.30}$$

which proves the proposition. □

Note that we implicitly assume here that λ_b is chosen such that $P_a + \Phi < P_{po}$ so that if $P_{wdes}(t)$ remains above P_{po}, then P_w remains above P_a and the system performance is unaffected by the limit on $\frac{\partial P_w}{\partial V}$.

4.3.3 Estimating t_s

While mathematically satisfying, a guarantee that the brake controller will begin to track in finite time does not mean much to a passenger waiting for braking to commence. It would be far better if the bounds on the time above were sufficiently tight to compute a reasonable estimate on this time. As written, these bounds can be used for this purpose, but putting an additional assumption on the brake trajectory allows for an even better estimation of the performance.

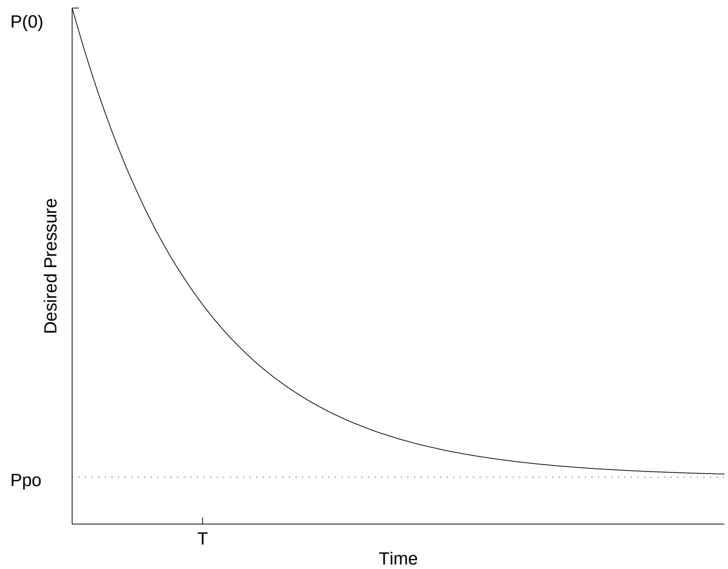

Figure 4.4: Trajectory Producing Maximum t_s

Assumption 4 (Initially Nondecreasing Trajectory) *The desired brake pressure profile is nondecreasing in the finite period of time before tracking as a sliding controller commences.*

The reason for this assumption is to remove the $[\bar{P}(0) - P_{po}]$ terms from the estimate on the time. These terms arise from behavior such as that illustrated in Figure 4.4, where the desired brake pressure is given by

$$P_{wdes} = (P(0) - P_{po})\, e^{-t/T} + P_{po} \tag{4.31}$$

Since the derivative of this function is

$$\dot{P}_{wdes} = -\frac{1}{T}\,(P(0) - P_{po})\, e^{-t/T} \tag{4.32}$$

the controller sees the initial error in the desired wheel pressure, but is also fed a negative value of $\dot{P}_{wdes}$. Since the integral of the desired pressure trajectory contributes to the displaced volume, this term tends to decrease the volume displaced. Of course, there is a limit on how low the desired pressure can fall under Assumption 1, so this integral can cause only a finite increase in the time required to reach P_a. This limit is given by the $[\bar{P}(0) - P_{po}]$ terms in the time estimate which reflect the limiting case as $T \to 0$ in Equation 4.31.

Within the context of braking, this is a rather artificial trajectory. In general, if the brake pressure has not reached P_{po}, the desired amount of braking will not decrease. This of course assumes that the time required to begin tracking is small, relative to the frequency of desired acceleration signals. We will therefore accept Assumption 4, calculate the bound on time that results and check to see if this assumption is reasonable in the context of the problem. While this may seem somewhat circular, this analysis is intended as a reasonable *estimate* of the time required to transition to sliding control; the bound of Proposition 1 still holds for the general case.

Proposition 3 (Estimate of t_s) *Under Assumptions 1 and 4, and the controller structure in Equations 4.8 to 4.10, the time required for sliding control to commence is bounded by:*

$$t \leq \frac{V_o a}{\lambda_b P(0)} + \frac{(V_a - V_o)a}{\lambda_b (P(0) - P_a)}$$

Proof As mentioned above, the main purpose of Assumption 4 is to eliminate the $[\bar{P}(0) - P_{po}]$ terms. Indeed, if $P_{wdes}(t)$ is nondecreasing, then:

$$\int_0^t \dot{P}_{wdes} dt \geq 0 \tag{4.33}$$

Equation 4.19 becomes

$$t_1 \leq \frac{V_o a}{\lambda_b P(0)} \doteq \bar{t}_1 \tag{4.34}$$

and Equation 4.22 becomes

$$t_2 \leq \bar{t}_1 + \frac{(V_a - V_o)a}{\lambda_b (P(0) - P_a)} \tag{4.35}$$

which proves the proposition. □

A similar result holds for the uncertain case. Note that by calculating t_2 with the smallest possible pressure difference below P_a, namely $P_{po} - P_a$, this bound is still on the conservative side. Evaluating these bounds in terms of the physical system parameters (see Section 4.5), however, gives $t_1 \leq 6$ms and $t_2 \leq 143$ms. The "pure" time delay in system response is therefore only 6 milliseconds while the 143 millisecond figure quantifies the the effect of limiting $\frac{\partial P_w}{\partial V}$ on our ability to make performance guarantees. Tracking may be (and, in practice, is) very good during this period, but the ability to make definitive statements is limited. On the time scale of general automated highway maneuvers, however, 143 milliseconds is a very short period (for further justification of this, see the simulations in the following chapter), so this limitation is quite minor.

4.4 Saturated Sliding Controller

Since the desired wheel pressure must always be greater than the push-out pressure, the initial error seen by the sliding controller is finite. Increasing λ_b to reject errors in the parameters, therefore, can produce a large initial control activity. This grows to be an even greater problem when hysteretic switching is employed and the first brake pressure commanded must be even greater than P_{po}. In cases where such high levels of control are undesirable, a saturated sliding mode controller can be used.

In this formulation, the reaching phase of the sliding controller is governed by:

$$\dot{S}_b = -K\text{sat}\left(\frac{S_b}{\Phi}\right) \tag{4.36}$$

as opposed to Equation 4.5. The saturation function, sat(), is defined to be:

$$\text{sat}\left(\frac{S_b}{\Phi}\right) = \begin{cases} \frac{S_b}{\Phi} & S_b > \Phi \\ 0 & \text{otherwise} \end{cases} \tag{4.37}$$

Using the same limit on $\frac{\partial P_w}{\partial V}$ as in Section 4.2 (Equation 4.10), the equations for the commanded master cylinder pressure are given by:

$$\dot{P}_{wdes} > \lambda_b(P_w - P_{wdes}) \implies P_{mc} = P_w + \left(\frac{\dot{P}_{wdes} - K\text{sat}\left(\frac{S_b}{\Phi}\right)}{\frac{\delta P_w}{\delta V} C_q}\right)^2 \tag{4.38}$$

$$\dot{P}_{wdes} < \lambda_b(P_w - P_{wdes}) \implies P_{mc} = P_w - \left(\frac{\dot{P}_{wdes} - K\text{sat}\left(\frac{S_b}{\Phi}\right)}{\frac{\delta P_w}{\delta V} C_q}\right)^2 \tag{4.39}$$

$V_o = 0.22\,\mathrm{cm}^3$	$P_a = 85\,\mathrm{kPa}$	$C_q = 1.49\,\mathrm{cm}^3/\mathrm{s}\sqrt{\mathrm{kPa}}$
$V_a = 1.47\,\mathrm{cm}^3$	$P_{po} = 115\,\mathrm{kPa}$	$a = 137\mathrm{kPa}/\mathrm{cm}^3$

Table 4.1: Brake Hydraulic Parameters Used in Simulations

Within the boundary layer determined by $|S_b| \leq \Phi$, the controller functions exactly as the controller in the previous section. Outside this boundary layer, however, the saturation function minimizes the amount of control activity. This change in structure does alter the controller performance, somewhat, but the essential performance guarantees remain. Indeed, results analogous to Propositions 1 to 3 can be made for this controller. Since the linear sliding controller of Section 4.2 fits more closely with the vehicle control framework presented in the following chapters and the initial control activity can be limited by judicious choice of P_a, we will use the linear form in the remainder of the thesis.

4.5 Simulation Results

This section provides a graphical interpretation of the controller performance by illustrating simulation results of the closed-loop brake controller. In these simulations, the brake fluid capacity curve used was

$$P_w(V) = \begin{cases} -1.0858V^3 + 57.737V^2 - 2.2421V + 0.02177 & V > V_o \\ 0 & V \leq V_o \end{cases} \tag{4.40}$$

which represents a polynomial fit to experimental data. Additional parameters are shown in Table 4.1. The simulations were all performed using a fourth-order Runge-Kutta integration algorithm with a fixed step size of 1 millisecond. Figure 4.5 shows the controller performance while tracking a sinusoidal trajectory. As the sliding controller formulation guarantees, the tracking error after the initial pressure rise is solely the result of the finite sampling time in the simulation.

In the experimental system, however, the controller sampling time, t_c, ranges between 5 and 10 milliseconds and the value of $\dot{P}_{wdes}$ is approximated for calculation purposes by $\frac{\Delta P_{wdes}}{t_c}$. Figure 4.6 shows the controller

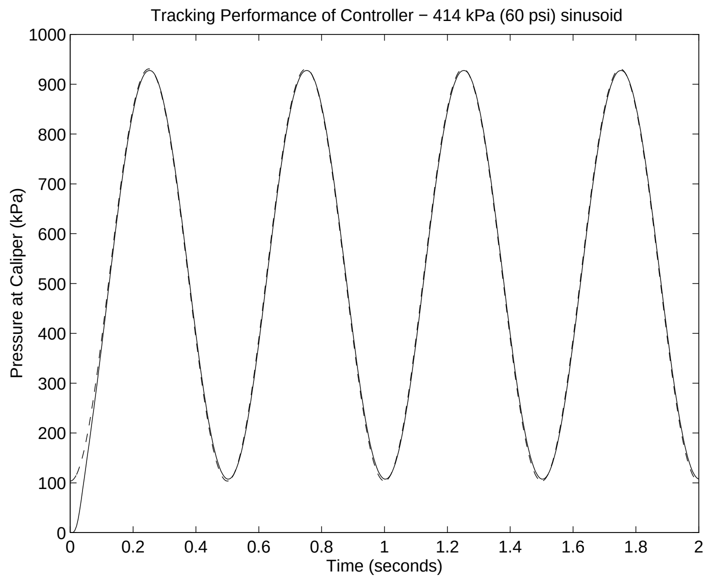

Figure 4.5: Simulated Performance: 1ms Update (Desired - dashed, Actual - solid)

performance for various amplitude signals when these factors are included in the simulation. From an application standpoint, the peak values of these three signals represent decelerations of about 0.08g to 0.15g (assuming that drag forces associated with highway speeds also act on the vehicle). Note that despite the variation of the fluid capacity curve over this range of pressures, the tracking accuracy is quite uniform as a result of the nonlinear control law. Furthermore, the controller sampling time introduces little error.

Of course, large gains can often produce excellent tracking performance at the expense of very high control activity. Figure 4.7, however, illustrates the master cylinder pressure required to produce this lead compensation for the brake hydraulics. Because of the limit on $\frac{\partial P_w}{\partial V}$, the initial master cylinder pressure is not large; rather, it is limited to a very reasonable value below 500 kPa. Thus, these tracking results are not the product of abnormally large master cylinder pressure commands. Indeed, after the initial filling period, the master cylinder pressure appears very nearly sinusoidal.

Neither do these results require very accurate knowledge of the system parameters. Robustness to uncertainty in V_o and V_a is, of course, inherent

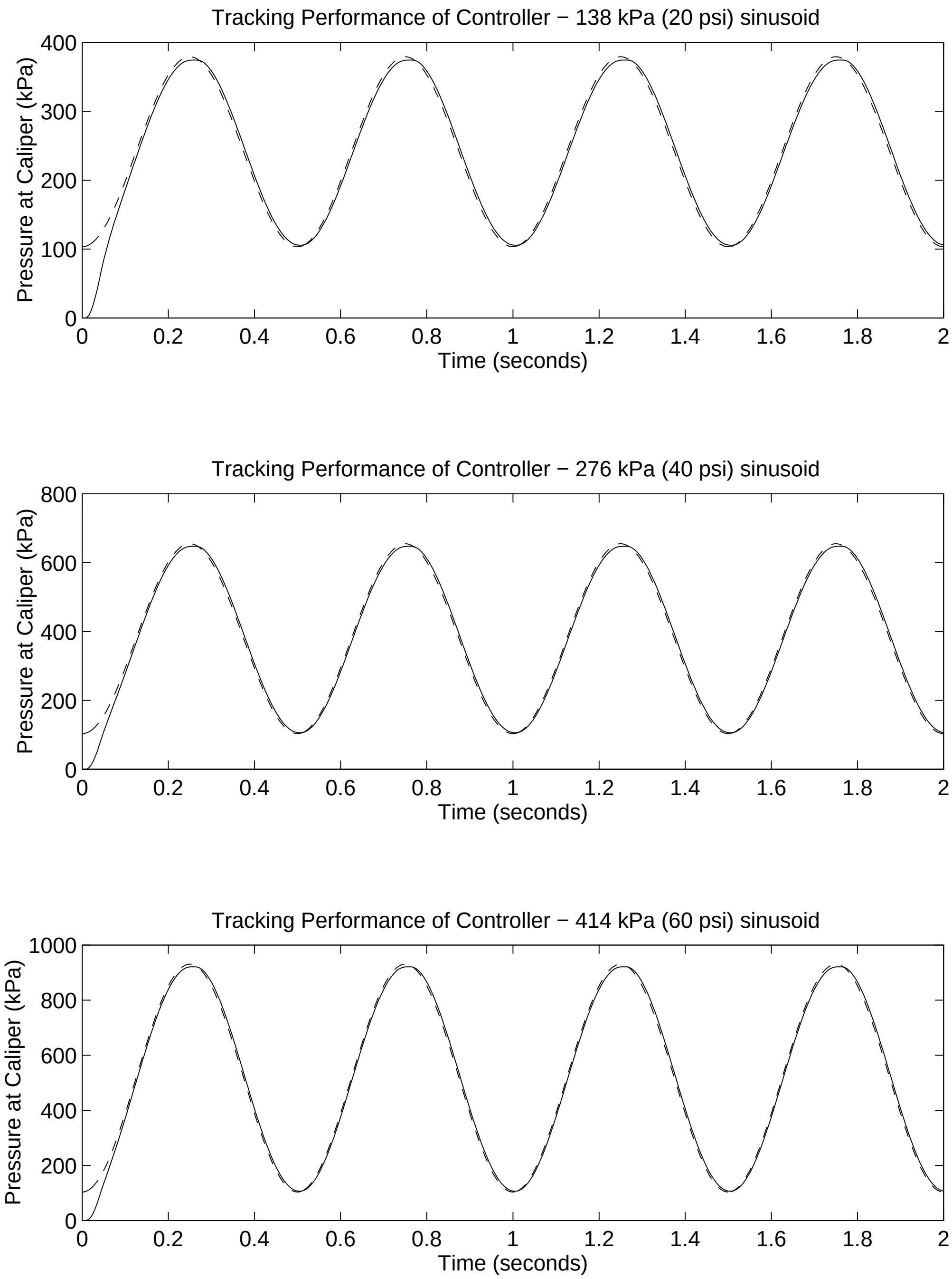

Figure 4.6: Simulated Performance: 5ms Update (Desired - dashed, Actual - solid)

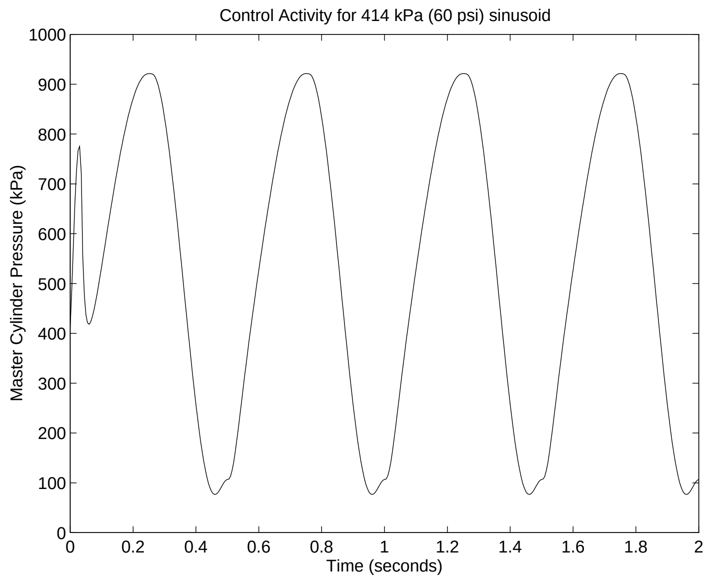

Figure 4.7: Control Activity with 5ms Controller Update

in the design, since the controller relies solely on pressure feedback. Furthermore, as Figure 4.8 illustrates, even 20% errors in the modeled value of the flow coefficient produce little tracking error. Because errors in the slope $\frac{\partial P_w}{\partial V}$ behave similarly, these were not simulated separately.

4.6 Experimental Results

The simulations, while encouraging, assume that the master cylinder pressure can be treated as a control input. In reality, the actuation system of Section 4.1 possesses some (nonlinear) dynamics which may be expected to impede the performance. Thus the true test remains whether or not this controller works when implemented on the experimental system.

Figure 4.9 shows the tracking performance of the experimental system for the sinusoidal profiles of Figure 4.6. The results are quite close to those predicted by the simulation, especially with respect to tracking error and the initial pressure rise exhibited by the system. The one discrepancy is the oscillatory nature of the pressure as the tracking error first approaches zero. The cause of this can be traced to the master cylinder pressure - shown in

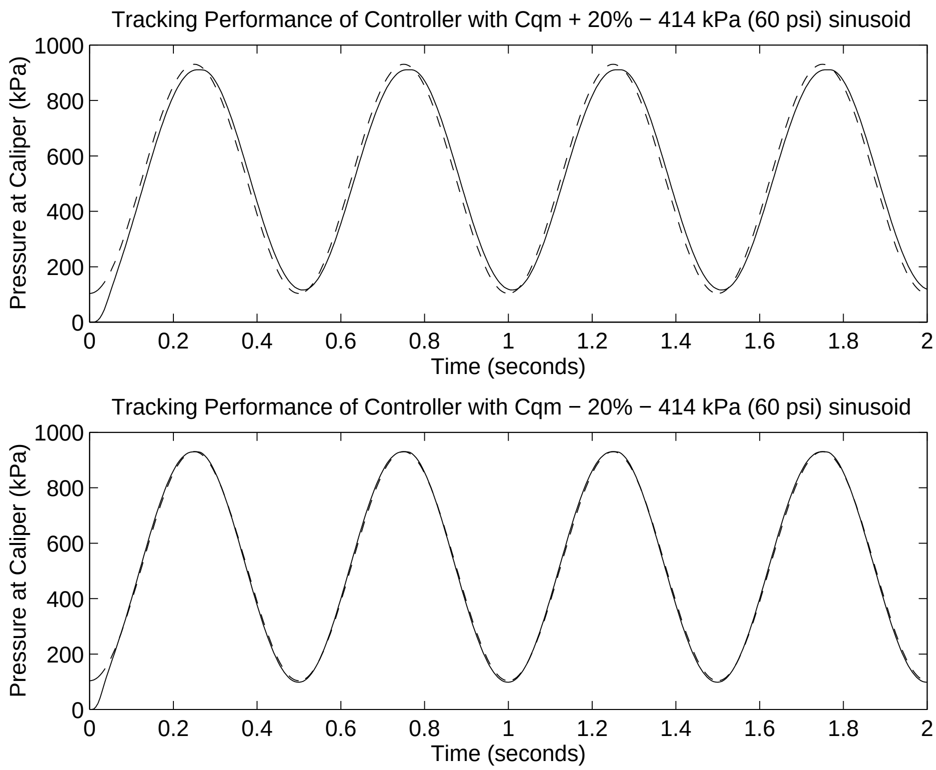

Figure 4.8: Simulated Performance: Uncertainty (Desired - dashed, Actual - solid)

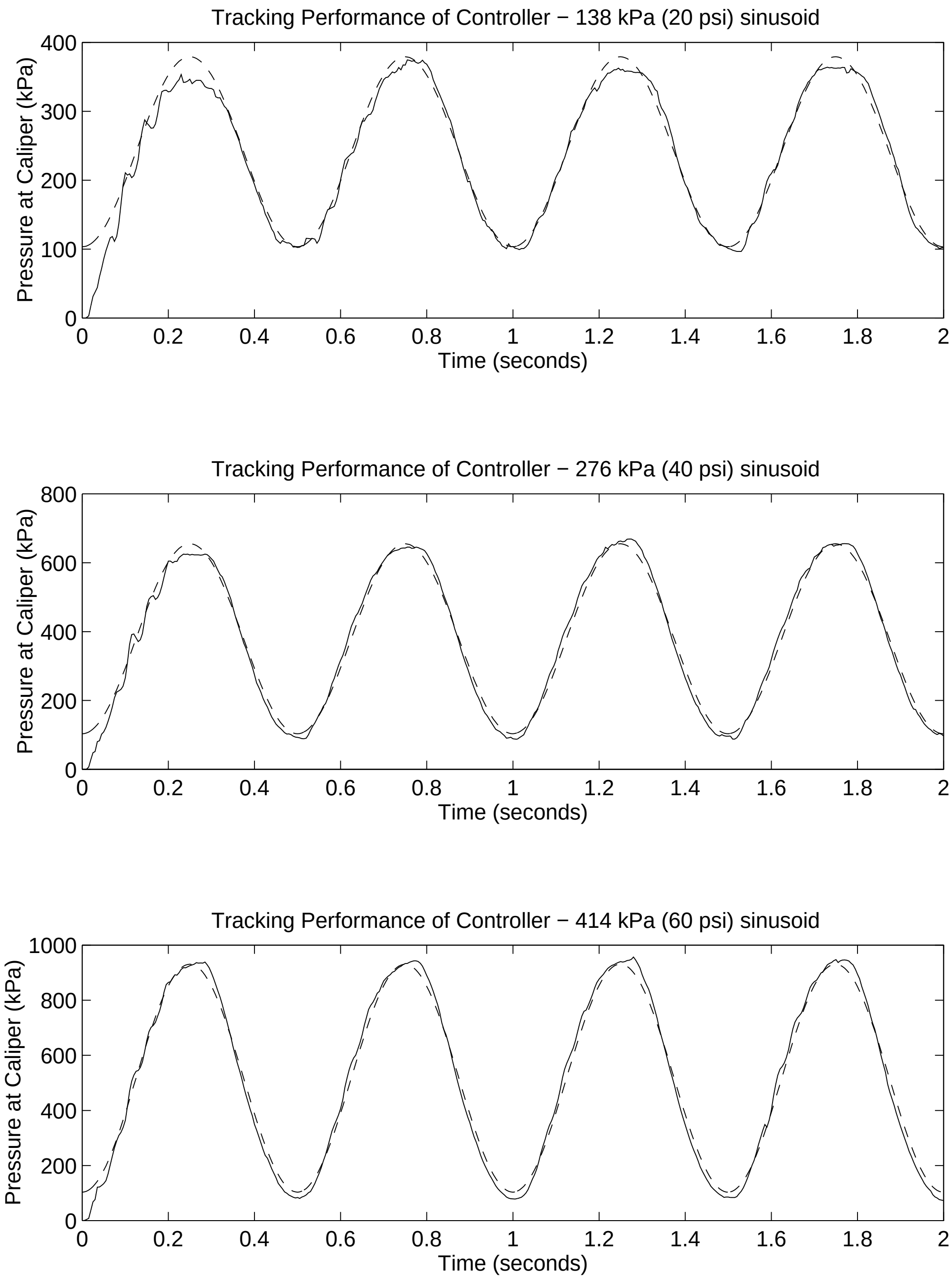

Figure 4.9: Experimental Controller Performance (Desired - dashed, Actual - solid)

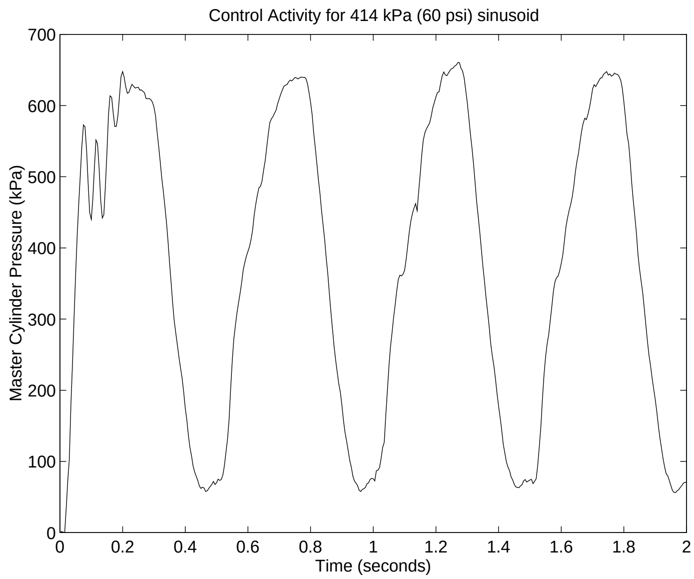

Figure 4.10: Control Activity During Tracking

Figure 4.7 for the 414 kPa sinusoid - and the neglected actuator dynamics. Because of the single-acting hydraulic cylinder, a decrease in the master cylinder pressure entails switching from supply pressure to tank, therefore involving valve hysteresis and master cylinder seal friction. These factors prevent the rapid pressure changes produced in simulation (which are not necessarily smooth, due to the square root nonlinearity) and induce these small fluctuations.

While these effects seem quite pronounced for the 138 kPa amplitude trajectory, it is important to keep magnitudes in perspective. The peak deceleration resulting from this particular trajectory is a mere 0.08g, below the threshold at which most people can even sense deceleration. Additionally, the pressure sensors used for the wheel and master cylinder pressures must be able to withstand a full application of the brakes without bursting and, therefore, range from 0-1000 psi (0 - 6895 kPa). Hence, the fluctuations represent less than 1% of the sensor range and fall well within the magnitude of sensor noise. Furthermore, the trajectories shown here tend to highlight this effect. The 2Hz signals above have much larger peak values of $\dot{P}_{wdes}$ than do the trajectories produced by the vehicle controller. As a result, in vehicle control testing, such behavior is indistinguishable from sensor noise, if it appears at all. Therefore, while the actuator could be re-designed to reduce this behavior, there is no particular motivation for doing so and plenty of safety-related arguments against other designs.

Chapter 5

Conclusions

The California PATH program has been conducting research in the area of vehicle control systems for application to an automated highway system. This research has been in many of the enabling technologies, such as sensors and actuators, as well as in longitudinal and lateral control algorithms. PATH has recently become part of the NAHSC to evaluate the feasibility of an AHS. A technology demonstration, currently being planned for 1997, should showcase many of the technologies described in this report.

This report has demonstrated, through simulation, the need for accurate brake torque control to ensure tight tracking and comfort in a platoon of vehicles. As a result of these simulations, we conclude that an actuation scheme capable of providing acceptable performance must bypass the booster, include some mechanism for torque feedback and eliminate time delays in the response. While such requirements are strict, they are nevertheless feasible, and may be achieved either through actuating the master cylinder or modulating the brake pressure directly.

Based upon these results, we have designed a master cylinder actuator and will soon begin testing in a vehicle control context. Current implementation issues with this system include incorporating a nonlinear first-order model of the brake hydraulics into the sliding controller and eliminating undesired switching between throttle and brakes due to sensor noise.

While the brake controller presented here clearly performs as desired, it is by no means the final word on the subject. From a hardware standpoint, actuating at the master cylinder is not a reasonable strategy as far as production is concerned. Hence, actuation through more readily manufactured means (such as ABS or TCS hardware) is a logical step. As mentioned before, the proposed algorithm should also work with this hardware. An interesting question, however, is whether or not linearization of the dynamics in this manner represents the best control strategy. While building the square-root flow law into the controller accurately reflects the system dynamics, it creates a nonsmooth control signal, potentially exciting unmodeled dynamics. Thus the benefits of such an approach depend highly upon the actuator speed. Finally, feedback of the brake torque would increase the robustness of the vehicle controller by moving this error to the lower (and faster) surface. Measurement of the torque and design of a controller to utilize this feedback, however, are decidedly non-trivial and represent another avenue for investigation.

Bibliography

AHS-System Objectives and Characteristics, Final Draft (1995). Technical report. National Automated Highway System Consortium (NAHSC). 3001 West Big Beaver Rd., Suite 500, Troy, MI.

Chien, C. C. and P. Ioannou (1992). Automatic vehicle following. In: *Proceedings of the 1992 American Control Conference, Chicago, IL.*

Choi, S.-B. and J.K. Hedrick (1995). Vehicle longitudinal control using an adaptive observer for avhs. In: *Proceedings of the 1995 ACC*. Seattle, WA.

Foreman, B. (1995). A survey of wireless communications technologies for automated vehicle control. In: *SAE FTT Conference*. SAE. Costa Mesa, CA.

Gerdes, Christian (1996). Decoupled Design of Robust Controllers for Nonlinear Systems: As Motivated by and Applied to Coordinated Throttle and Brake Control for Automated Highways. PhD thesis. University of California at Berkeley. Berkeley, CA.

Gerdes, J. C., A. S. Brown and J. K. Hedrick (1995). Brake system modeling for vehicle control. In: *Advanced Automotive Technologies - 1995 ASME IMECE*. pp. 105–112.

Gerdes, J. C. and J. K. Hedrick (1995*a*). Brake system requirements for platooning on an automated highway. In: *Proceedings of the 1995 American Control Conference, Seattle, WA*. pp. 165–169.

Gerdes, J. C., D. B. Maciuca, J. K. Hedrick and P. E. Devlin (1993). Brake system modeling for IVHS longitudinal control. In: *Advances in*

Robust and Nonlinear Control Systems, ASME *Winter Annual Meeting.* pp. 119–126.

Gerdes, J.C. and J.K. Hedrick (1995*b*). Brake system requirements for platooning on an automated highway. In: *Proceedings of the 1995 American Control Conference (ACC).* Seattle, WA.

Hedrick, J. K., D. McMahon, V. Narendran and D. Swaroop (1991). Longitudinal vehicle controller design for IVHS systems. In: *Proceedings of the 1991 American Control Conference, Boston, MA.* pp. 3107–3112.

Hedrick, J.K. (1995). Vehicle control issues in Intelligent Vehicle Highway Systems. 1st IFAC Workshop on Advances in Automotive Control. Ascona, Switzerland.

Hedrick, J.K. and D. Swaroop (1993). Dynamic coupling in vehicles under automatic control. In: *Proceedings of the 13th IAVSD Symposium.* Chendu, China.

Hedrick, J.K., M. Tomizuka and P. Varaiya (1994). Control issues in Automated Highway Systems. *IEEE Control Systems Magazine.*

Hsu, A., F. Eskafi, S. Sachs and P. Varaiya (1993). Protocol design for an automated highway system. *Discrete Event Dynamic Systems* **2**, 183–206.

Hurtig, J. K., S. Yurkovich, K. M. Passino and D. Littlejohn (1994). Torque regulation with the General Motors ABS VI Electric Brake System. In: *Proceedings of the 1994 American Control Conference, Baltimore, MD.*

Ioannou, P. and Z. Xu (1994). Throttle and brake control systems for automatic vehicle following. *IVHS Journal* **1**(4), 345–377.

Maciuca, D. B., J. C. Gerdes and J. K. Hedrick (1994). Automatic braking control for IVHS. In: *Proceedings of the International Symposium on Vehicle Control.*

McMahon, D. H., J. K. Hedrick and S. E. Shladover (1990). Vehicle modelling and control for automated highway systems. In: *Proceedings of the 1990 American Control Conference, San Diego, CA.* pp. 297–303.

McMahon, D. H., V. K. Narendran, D. Swaroop, J. K. Hedrick, K. S. Chang and P. E. Devlin (1992). Longitudinal vehicle controllers for IVHS: Theory and experiment. In: *Proceedings of the 1992 American Control Conference, Chicago, IL.* pp. 1753–1757.

Peng, H., W.B. Zhang, S. Shladover, M. Tomizuka and A. Arai (1993). Magnetic-marker-based lane keeping: A robust experimental study. *SAE* (SAE Paper No. 930556), 127–132.

Perronne, J-M., M. Renner and G. L. Gissinger (1994). Dynamic aspects of a calliper brake system. In: *Proceedings of the International Symposium on Vehicle Control.*

Radlinski, R. W. (1991). The effect of aftermarket linings on light vehicle braking performance. Final Report DOT HS 807 835. U.S. Department of Transportation, NHTSA.

Ranging Sensors for Use in Longitudinal Control Research (1995). Technical Report RFP Sensor/BC. PATH.

Reichart, G. and K. Naab (1994). Systems for lateral and longitudinal vehicle guidance. In: *Proceedings 1st World Congress on Applications of Transport Telematics and Intelligent Vehicle-Highway Systems.* Paris, France.

Ren, W. and D. Green (1994). Continuous platooning: A new evolutionary and operating conception for automated highway systems. In: *Proceedings of the 1994 American Control Conference, Baltimore, MD.*

Shladover, S. (1995). Review of the state of development of advanced vehicle control systems. *Vehicle System Dynamics.*

Shladover, S.E. and et. al. (1991). Automatic vehicle control developments in the PATH program. *IEEE Transactions on Vehicular Technology* **40**(1), 114–130.

Slotine, Jean-Jacques E. and Weiping Li (1991). *Applied Nonlinear Control.* Prentice Hall. Englewood Cliffs, NJ.

Stevens, W.B. (1993). The ahs concepts analysis. Technical Report MTRW0000123. MITRE. McLean, Va.

Swaroop, D. and J. K. Hedrick (1994). Direct adaptive control of vehicle platoons. In: *Proc. 33rd CDC, Lake Buena Vista, FL.* pp. 684–689.

Tomizuka, M. and J.K. Hedrick (1995). Advanced control methods for automotive applications. *Vehicle System Dynamics.*

van Zanten, Anton T., Rainer Erhardt and Georg Pfaff (1995). VDC, the vehicle dynamics control system of Bosch. SAE Paper # 950759.

Varaiya, P. (1993). Smart cars on smart roads: Problems of control. In: *IEEE Transactions on Automatic Control.* Vol. 38. IEEE.